



OPEN Exploring the wave's structures to the nonlinear coupled system arising in surface geometry

Khizar Farooq¹, Ejaz Hussain², Usman Younas³, Herbert Mukalazi⁴✉, Tamer M. Khalaf⁵, Abdul Mutlib¹ & Syed Asif Ali Shah^{6,7,8}

This manuscript deals with the Heisenberg ferromagnet-type integrable Akbota equation (AE), which refers to a set of differential equations that are integrable and linked together, and they possess solitary waves. AE is a basic gear for investigating nonlinear dynamics in the fields of optics, magnetism, and differential geometry of curves and surfaces. It is extensively used to represent optical solitons in nonlinear optical fibers, which are crucial for fiber-optic communication owing to their capacity to maintain form across considerable distances. The dynamical behavior of AE is explored by constructing accurate closed-form traveling wave solutions. For this purpose, the Kumar-Malik method, the new Kudryashov method, and the Riccati equation method are utilized. The resulting solutions consist of trigonometric, hyperbolic, and rational functions. By employing these methodologies, precise analytical remedies for soliton waves are derived, which include kink, bright, and dark solitons. To get a better understanding of the physical aspects of these solutions, we depict them via several visual representations. 3D-surface graphs, 2D-line graphs, and contour and density plots, in addition to theoretical derivations.

Keywords Akbota equation, Kumar–Malik method, New Kudryashov method, Riccati equation method, Exact solutions

In the area of scientific inquiry, scientists are increasingly intrigued by the subtle dynamics of natural occurrences. Leveraging cutting-edge approaches and procedures, they attempt to decode these complexities with more accuracy and insight. An important tool in this effort is the use of partial differential equations (PDEs) to create models that correctly capture these events. The expanding capacity of 3D visualization plays a crucial role in boosting researchers' knowledge and analysis of such occurrences. By applying PDEs, scientists are able to reveal the complicated patterns controlling physical processes and give greater insights into their behavior.

A soliton is an isolated solitary wave that propagates over a material without wasting energy or altering its shape due to contact with other waves. Solitons are distinct from regular wave occurrences due to their strong localization and remarkable stability and endurance. Soliton plays a crucial role in several disciplines of study such as nonlinear optics^{1,2}, mechanics³, plasma physics⁴, engineering⁵, hydrodynamics⁶, communication systems⁷, optical fiber⁸, biology⁹, fluid dynamics^{10,11}.

Nonlinear partial differential equations (NLPDEs) grow as exceptionally crucial assets in this scientific pursuit. NLPDEs provide sophisticated insights into a wide range of fields, including optics, acoustics, plasma dynamics, and condensed matter physics. They not only increase our comprehension of the researched events but also allow scientists to make precise estimates about their future proliferation. As a result, many academics have committed to analyzing diverse NLPDEs, seeking to expand their comprehension of the exhibited behavior in the examined natural occurrences. Recent assessments have involved inquiries into the Batman–Burger equation^{12,13}, Schrodinger equation^{14–18}, Date–Jimbo–Kashiwara–Miwa equation^{19–21}, thin film ferroelectric material equation^{22–25}, Benjamin–Bona–Mahony equation^{26–28}, Boussinesq equation^{29–32}, generalized Calogero–

¹Centre for High Energy Physics, University of the Punjab, Quaid-e-Azam Campus, Lahore 54590, Pakistan.

²Department of Mathematics, University of the Punjab, Quaid-e-Azam Campus, Lahore 54590, Pakistan.

³Department of Mathematics, Shanghai University, No. 99 Shangda Road, Shanghai 200444, China. ⁴Department of Mathematics and Statistics, Faculty of Science, Kyambogo University, Kampala, Uganda. ⁵Department of Industrial Engineering, College of Engineering, King Saud University, Riyadh 12372, Saudi Arabia. ⁶Department of Modern Mechanics, School of Engineering Science, University of Science and Technology of China, Hefei 230026, China.

⁷Jinhua Hangda Beidou Applied Technology Co., Ltd., Jinhua 321004, China. ⁸Department of Mathematics and Statistics, The University of Lahore, 1-km Defence Road, Lahore 54000, Pakistan. ✉email: hmukalazi@kyu.ac.ug

Bogoyavlenskii-schiff equation^{33,34}, Buckmaster equation³⁵, non-linear non classical Sobolev-type wave model³⁶, and different other^{37–49}.

The study of the single-wave solutions of NLPDEs is significant for giving better views and understanding of the underlying process and useful uses. Therefore, numerous researchers have created new ways to study these NLPDEs answers. Plenty of strong techniques such as, $\exp(-\chi(\Theta))$ expansion method⁵⁰, extend mapping method⁵¹, homotopy perturbation method⁵², Darboux transformation⁵³, exp-function method⁵⁴, generalized Kudryashov method⁵⁵, extended trial equation method⁵⁶, Hirota bilinear method⁵⁷, extended jacobian method⁵⁸, extended direct algebraic method⁵⁹, improved extended fan-sub equation method⁶⁰, modified extended tanh method, Backlund transform method⁶¹, Novel $(\frac{G'}{G})$ expansion method⁶², extended auxiliary equation mapping method⁶³, extended simple equation method⁶⁴ and many more methods^{65–71}.

In this work, we shall analyze the AE

$$\begin{aligned} IU_t + a U_{xx} + b U_{x,t} + \gamma SU &= 0, \\ S_x - 2\epsilon(a|U|_x^2 + b|U|_t^2) &= 0, \epsilon = \pm 1 \end{aligned} \quad (1)$$

here $S = S(x,t)$ is a real-valued function and $U = U(x,t)$ is a complex function and a, b and γ are arbitrary constants. The AE represents a generalized form of the two additional equations that can be derived from it:

- When a equals zero, AE becomes the Kuralay equation.
- When b equals zero, AE becomes the Schrodinger equation.

The Darboux transformation approach yields many wave solutions, including breather, rogue wave, and semi-rational solutions to the AE, as shown by Kong and Guo⁷². Sagidullayeva et al.⁷³ derive the Lax representations and their gauge equivalent substitutes for AE. The New Extended Auxiliary Equation (NEAE) approach (Mathanaranjan et al.⁷⁴; Zayed and Alurfi⁷⁵) is used to get the soliton solutions of the auxiliary equation. Zhao Li and Shan Zhao researched the dynamical behavior and soliton solutions of the AE based on the analytical approach of the planar dynamic system⁷⁶. The AE is characterized as a Heisenberg ferromagnet-type equation, playing a significant role in the study of nonlinear dynamics in magnetism, the differential geometry of surfaces and curves, and optics. Analytical solutions serve as crucial instruments in scientific research as well as technical applications. Not only do they increase our knowledge of natural processes, but they also offer a robust framework for theoretical growth, allowing accurate control and prediction of systems. Due to its extensive application across multiple scientific areas, getting analytical answers is important to unlocking the full potential of the AE model. These solutions give a clear and straightforward picture of the interactions between parameters and variables, making it easy to fully appreciate the underlying behavior of the systems the equations describe. They also give a more thorough knowledge of the fundamental principles controlling these complicated structures.

This paper investigates solutions of soliton waves of the understudied model using the Kumar-Malik method Riccati equation method and the new Kudryashov method. Particularly, research on this specific question has not been done in the existing literature. The utilization of such processes gives a broad variety of options, such as incorporating bright, dark, and kink solitons. The usefulness of these strategies has been shown in solving various models in the accessible research.

The full article is summarized as follows: “Reduction of proposed model into ODE” explains the mathematical analysis needed to convert the nonlinear partial differential problem to an ordinary differential equation. “Description of Kumar–Malik method” discusses the mathematical processes of the Kumar–Malik method, and its application, and gives graphical representations. “The new Kudryashov method” describes the new Kudryashov method and its application. “Riccati equation method” discusses the mathematical processes of the Riccati Equation method and its application. “Graphical representation and discussion” discusses the graphical representation and discussion of the obtained results. Finally, “Conclusion” closes the work.

Reduction of proposed model into ODE

Consider general NLPDEs have the following form:

$$Y(U, U_t, U_x, U_{t,t}, U_{x,x}, \dots) = 0. \quad (2)$$

Its non linear ordinary differential equations (NLODEs) will be

$$P(\Phi, \Phi', \Phi'', \dots) = 0. \quad (3)$$

Consider the traveling ansatz solution to simplify the NLPDEs into NLODEs.

$$U(x, t) = \Phi(\xi)e^{i(kx - \omega t)}, \quad S(x, t) = g(\xi); \quad \xi = x - \eta t. \quad (4)$$

here ω, k and η are the constants. Inserting Eq. (4) into Eq. (1) and separating the real and Imaginary parts we obtained the following equation:

$$(-n^2\delta - \omega + n\theta\omega + \gamma g(\xi)) \Phi(\xi) + (\delta - \theta\eta)\Phi''(\xi) = 0. \quad (5)$$

$$(-2n\delta - \eta + n\theta\eta + \theta\omega) \Phi'(\xi) = 0. \quad (6)$$

$$4\epsilon(\delta - \theta\eta)\Phi(\xi)\Phi'(\xi) + g'(\xi) = 0. \quad (7)$$

From Eq. (6), we get

$$\omega = \frac{2n\delta + \eta - n\theta\eta}{\theta}. \tag{8}$$

Integrating Eq. (7) w.r.t ξ and assuming the integration constant zero, we get:

$$g(\xi) = 2\epsilon(\delta - \theta\eta)\Phi(\xi)^2. \tag{9}$$

By substituting Eqs. (8,9) into Eq. (5), we attain:

$$(-\eta + n(-2 + n\theta)(\delta - \theta\eta))\Phi(\xi) + 2\theta\gamma\epsilon(\delta - \theta\eta)\Phi(\xi)^3 + \theta(\delta - \theta\eta)\Phi''(\xi) = 0. \tag{10}$$

here $(\delta - \theta\eta) \neq 0$.

Description of Kumar–Malik method

Following are the major steps of the Kumar–Malik method.

Step 01: The Kumar–Malik method provides the solution of Eq. (10) as:

$$\Phi(\xi) = B_0 + \sum_{i=1}^N B_i f(\xi)^i. \tag{11}$$

where the coefficients B_i 's ($i = 1, 2, \dots, N$) are constants, and the first-order differential equation is accomplished by the function $f(\xi)$ as:

$$f(\xi)' = \sqrt{\sigma_1 f(\xi)^4 + \sigma_2 f(\xi)^3 + \sigma_3 f(\xi)^2 + \sigma_4 f(\xi) + \sigma_5} \tag{12}$$

where σ_i 's, for ($i = 1, 2, \dots, N$) are constants. The solution to the Eq. (12) as follows:

Case 01: when $\sigma_4 := \frac{\sigma_2 k_1}{8\sigma_1^2}$, $\sigma_5 = 0$ then Eq. (12) has the following Jacobi elliptic solutions:

- If $\sigma_1 < 0, k_1 > 0$,

$$f_{01}(\xi) = -\frac{\sigma_2}{4\sigma_1} \pm \frac{\sigma_2}{4\sigma_1} \cdot \text{JacobiCN} \left[\frac{\sqrt{-\sigma_1 k_1}}{4\sigma_1} \xi, \frac{\sigma_2}{2\sqrt{k_1}} \right]. \tag{13}$$

$$f_{02}(\xi) = -\frac{\sigma_2}{4\sigma_1} \pm \frac{\sigma_2}{4\sigma_1} \cdot \text{JacobiDN} \left[\frac{\sigma_2}{4\sqrt{-\sigma_1}} \xi, \frac{2\sqrt{k_1}}{\sigma_2} \right]. \tag{14}$$

- If $\sigma_1 < 0, k_1 < 0, k_2 < 0$,

$$f_{03}(\xi) = -\frac{\sigma_2}{4\sigma_1} \pm \frac{\sqrt{-k_2}}{4\sigma_1} \cdot \text{JacobiCN} \left[\frac{\sqrt{\sigma_1 k_1}}{4\sigma_1} \xi, \frac{\sqrt{k_2 k_1}}{2k_1} \right]. \tag{15}$$

$$f_{04}(\xi) = -\frac{\sigma_2}{4\sigma_1} \pm \frac{\sqrt{-k_2}}{4\sigma_1} \cdot \text{JacobiDN} \left[\frac{\sqrt{\sigma_1 k_1}}{4\sigma_1} \xi, \frac{2\sqrt{k_2 k_1}}{k_2} \right]. \tag{16}$$

- If $\sigma_1 < 0, k_1 > 0, k_2 < 0$,

$$f_{05}(\xi) = -\frac{\sigma_2}{4\sigma_1} \pm \frac{\sqrt{-k_2}}{4\sigma_1} \cdot \text{JacobiNC} \left[\frac{\sqrt{-\sigma_1 k_1}}{2\sigma_1} \xi, \frac{\sigma_2}{2\sqrt{k_2}} \right]. \tag{17}$$

$$f_{06}(\xi) = -\frac{\sigma_2}{4\sigma_1} \pm \frac{\sqrt{-k_2}}{4\sigma_1} \cdot \text{JacobiND} \left[\frac{\sqrt{-\sigma_1 k_1}}{2\sigma_1} \xi, \frac{\sigma_2}{2\sqrt{k_2}} \right]. \tag{18}$$

- If $\sigma_1 k_1 > 0, k_1 k_2 > 0$,

$$f_{07}(\xi) = -\frac{\sigma_2}{4\sigma_1} \pm \frac{\sigma_2}{4\sigma_1} \cdot \text{JacobiNC} \left[\frac{\sqrt{\sigma_1 k_1}}{2\sigma_1} \xi, \frac{\sqrt{k_1 k_2}}{2k_1} \right]. \tag{19}$$

$$f_{08}(\xi) = -\frac{\sigma_2}{4\sigma_1} \pm \frac{\sigma_2}{4\sigma_1} \cdot \text{JacobiND} \left[\frac{\sqrt{\sigma_1 k_2} \cdot \xi}{2\sigma_1}, \frac{2\sqrt{k_1 k_2}}{k_2} \right]. \tag{20}$$

- If $\sigma_1 > 0, k_2 < 0$,

$$f_{09}(\xi) = -\frac{\sigma_2}{4\sigma_1} \pm \frac{\sigma_2}{4\sigma_1} \cdot \text{JacobiNS} \left[\frac{\sigma_2}{2\sqrt{\sigma_1}} \xi, \frac{\sqrt{-k_2}}{\sigma_2} \right]. \tag{21}$$

$$f_{10}(\xi) = -\frac{\sigma_2}{4\sigma_1} \pm \frac{\sqrt{-k_2}}{4\sigma_1} \cdot \text{JacobiNS} \left[\frac{\sqrt{-\sigma_1 k_2}}{4\sigma_1} \xi, \frac{\sigma_2}{\sqrt{-k_2}} \right]. \quad (22)$$

$$f_{11}(\xi) = -\frac{\sigma_2}{4\sigma_1} \pm \frac{\sqrt{-k_2}}{4\sigma_1} \cdot \text{JacobiSN} \left[\frac{\sigma_2}{2\sqrt{\sigma_1}} \xi, \frac{\sqrt{-k_2}}{\sigma_2} \right]. \quad (23)$$

$$f_{12}(\xi) = -\frac{\sigma_2}{4\sigma_1} \pm \frac{\sigma_2}{4\sigma_1} \cdot \text{JacobiSN} \left[\frac{\sqrt{-\sigma_1 k_2}}{4\sigma_1} \xi, \frac{\sigma_2}{\sqrt{-k_2}} \right]. \quad (24)$$

Case 02: when $\sigma_4 := \frac{\sigma_2 k_1}{8\sigma_1^2}$, $\sigma_5 = \frac{k_1^2}{64\sigma_1^3}$ then Eq. (12) has the following hyperbolic and trigonometric solutions:

- If $\sigma_1 > 0$, $k_3 < 0$,

$$f_{13}(\xi) = -\frac{\sigma_2}{4\sigma_1} \pm \frac{\sqrt{-k_3}}{4\sigma_1} \tanh \left[\frac{\sqrt{-\sigma_1 k_3}}{4\sigma_1} \xi \right]. \quad (25)$$

$$f_{14}(\xi) = -\frac{\sigma_2}{4\sigma_1} \pm \frac{\sqrt{-k_3}}{4\sigma_1} \coth \left[\frac{\sqrt{-\sigma_1 k_3}}{4\sigma_1} \xi \right]. \quad (26)$$

- If $\sigma_1 > 0$, $k_3 > 0$,

$$f_{15}(\xi) = -\frac{\sigma_2}{4\sigma_1} \pm \frac{\sqrt{k_3}}{4\sigma_1} \tan \left[\frac{\sqrt{\sigma_1 k_3}}{4\sigma_1} \xi \right]. \quad (27)$$

$$f_{16}(\xi) = -\frac{\sigma_2}{4\sigma_1} \pm \frac{\sqrt{k_3}}{4\sigma_1} \cot \left[\frac{\sqrt{\sigma_1 k_3}}{4\sigma_1} \xi \right]. \quad (28)$$

Case 03: when $\sigma_4 := \frac{\sigma_2 k_1}{8\sigma_1^2}$, $\sigma_5 = \frac{\sigma_2^2 k_2}{256\sigma_1^3}$ then we get the solution Eq. (12) has the following form:

- If $\sigma_1 < 0$, $k_3 < 0$,

$$f_{17}(\xi) = -\frac{\sigma_2}{4\sigma_1} \pm \frac{\sqrt{-2k_3}}{4\sigma_1} \operatorname{sech} \left[\frac{\sqrt{2\sigma_1 k_3}}{4\sigma_1} \xi \right]. \quad (29)$$

- If $\sigma_1 > 0$, $k_3 > 0$,

$$f_{18}(\xi) = -\frac{\sigma_2}{4\sigma_1} \pm \frac{\sqrt{2k_3}}{4\sigma_1} \operatorname{csch} \left[\frac{\sqrt{2\sigma_1 k_3}}{4\sigma_1} \xi \right]. \quad (30)$$

- If $\sigma_1 > 0$, $k_3 < 0$,

$$f_{19}(\xi) = -\frac{\sigma_2}{4\sigma_1} \pm \frac{\sqrt{-2k_3}}{4\sigma_1} \sec \left[\frac{\sqrt{-2\sigma_1 k_3}}{4\sigma_1} \xi \right]. \quad (31)$$

$$f_{20}(\xi) = -\frac{\sigma_2}{4\sigma_1} \pm \frac{\sqrt{-2k_3}}{4\sigma_1} \csc \left[\frac{\sqrt{-2\sigma_1 k_3}}{4\sigma_1} \xi \right]. \quad (32)$$

Case 04: when $\sigma_2 = \sigma_4 = \sigma_5 = 0$, $\sigma_3 > 0$ then we find out the solution Eq. (12) as:

$$f_{21}(\xi) = \frac{4\zeta\sigma_3}{4\zeta \exp(\sqrt{\sigma_3}\xi) - \sigma_1\sigma_3 \exp(-\sqrt{\sigma_3}\xi)}. \quad (33)$$

where

$$k_1 = 4\sigma_1\sigma_3 - \sigma_2^2, \quad k_2 = 16\sigma_1\sigma_3 - 5\sigma_2^2, \quad k_3 = 8\sigma_1\sigma_3 - 3\sigma_2^2. \quad (34)$$

Step 02: The value of N may readily be calculated by following the homogeneous balancing principle on Eq. (10).

Step 03: After putting the Eq. (11) and its derivatives according to the Eq. (12) in Eq. (10) the polynomials of $f(\xi)$ is obtained. After collecting all the coefficients of the different powers of $f(\xi)$ and equating to zero provides the system in the unknown parameters B'_i 's ($i = 1, 2, 3, \dots, N$), σ'_i 's ($i = 1, 2, 3, \dots, N$). Solving this set of algebraic equations yields the precise solution of Equation (1).

Solution by Kumar–Malik method

To obtain the solution of Eq. (10), find the value of positive integer $N=1$ and put it in Eq. (11), then Eq. (11) will become:

$$\Phi(\xi) = B_0 + B_1 f(\xi). \tag{35}$$

By inserting Eqs. (35) and (12) in Eq. (10) we obtained the set of algebraic equations by equating the different powers of $f(\xi)$ and then solving these equations for unknowns.

Set 1:

$$\delta = \eta \frac{8n^2\theta^2\sigma_1 + 8\theta^2\sigma_1\sigma_3 - 3\theta^2\sigma_2^2 - 16n\theta\sigma_1 + 8\sigma_1}{8n^2\theta\sigma_1 + 8\theta\sigma_1\sigma_3 - 3\theta\sigma_2^2 - 16n\sigma_1}, \quad B_0 = -\frac{\sigma_2}{4\rho\epsilon\sqrt{-\frac{\sigma_1}{\epsilon\rho}}}, \quad B_1 = \sqrt{-\frac{\sigma_1}{\epsilon\rho}} \tag{36}$$

By putting set 1 in Eq.(35) we obtained the exact solution as follows:

Case 01: when $\sigma_4 := \frac{\sigma_2 k_1}{8\sigma_1^2}, \sigma_5 = 0$ then Eq. (12) has the following Jacobi elliptic solutions:

- If $\sigma_1 < 0, k_1 > 0,$

$$U_{01}(\xi) = -\frac{\sigma_2}{4\rho\epsilon\sqrt{-\frac{\sigma_1}{\epsilon\rho}}} + \sqrt{-\frac{\sigma_1}{\epsilon\rho}} \left[-\frac{\sigma_2}{4\sigma_1} + \frac{\sigma_2 \cdot \text{JacobiCN}\left(\frac{\sqrt{-\sigma_1 k_1}}{4\sigma_1} \xi, \frac{\sigma_2}{2\sqrt{k_1}}\right)}{4\sigma_1} \right]. \tag{37}$$

$$U_{02}(\xi) = -\frac{\sigma_2}{4\rho\epsilon\sqrt{-\frac{\sigma_1}{\epsilon\rho}}} + \sqrt{-\frac{\sigma_1}{\epsilon\rho}} \left[-\frac{\sigma_2}{4\sigma_1} + \frac{\sigma_2 \cdot \text{JacobiDN}\left(\frac{\sigma_2}{4\sqrt{-\sigma_1}} \xi, \frac{2\sqrt{k_1}}{\sigma_2}\right)}{4\sigma_1} \right]. \tag{38}$$

- If $\sigma_1 < 0, k_1 < 0, k_2 < 0,$

$$U_{03}(\xi) = -\frac{\sigma_2}{4\rho\epsilon\sqrt{-\frac{\sigma_1}{\epsilon\rho}}} + \sqrt{-\frac{\sigma_1}{\epsilon\rho}} \left[-\frac{\sigma_2}{4\sigma_1} + \frac{\sqrt{-k_2} \cdot \text{JacobiCN}\left(\frac{\sqrt{\sigma_1 k_1}}{4\sigma_1} \xi, \frac{\sqrt{k_2 k_1}}{2k_1}\right)}{4\sigma_1} \right]. \tag{39}$$

$$U_{04}(\xi) = -\frac{\sigma_2}{4\rho\epsilon\sqrt{-\frac{\sigma_1}{\epsilon\rho}}} + \sqrt{-\frac{\sigma_1}{\epsilon\rho}} \left[-\frac{\sigma_2}{4\sigma_1} + \sqrt{-k_2} \cdot \text{JacobiDN}\left(\frac{\sqrt{\sigma_1 k_1}}{4\sigma_1} \xi, \frac{2\sqrt{k_2 k_1}}{k_2}\right) \right] / (4\sigma_1). \tag{40}$$

- If $\sigma_1 < 0, k_1 > 0, k_2 < 0,$

$$U_{05}(\xi) = -\frac{\sigma_2}{4\rho\epsilon\sqrt{-\frac{\sigma_1}{\epsilon\rho}}} + \sqrt{-\frac{\sigma_1}{\epsilon\rho}} \left[-\frac{\sigma_2}{4\sigma_1} + \sqrt{-k_2} \cdot \text{JacobiNC}\left(\frac{\sqrt{-\sigma_1 k_1}}{2\sigma_1} \xi, \frac{\sigma_2}{2\sqrt{k_2}}\right) \right] / (4\sigma_1). \tag{41}$$

$$U_{06}(\xi) = -\frac{\sigma_2}{4\rho\epsilon\sqrt{-\frac{\sigma_1}{\epsilon\rho}}} + \sqrt{-\frac{\sigma_1}{\epsilon\rho}} \left[-\frac{\sigma_2}{4\sigma_1} + \sqrt{-k_2} \cdot \text{JacobiND}\left(\frac{\sqrt{-\sigma_1 k_1} i}{2\sigma_1} \xi, \frac{\sigma_2}{2\sqrt{k_2}}\right) \right] / (4\sigma_1). \tag{42}$$

- If $\sigma_1 k_1 > 0, k_1 k_2 > 0,$

$$U_{07}(\xi) = -\frac{\sigma_2}{4\rho\epsilon\sqrt{-\frac{\sigma_1}{\epsilon\rho}}} + \sqrt{-\frac{\sigma_1}{\epsilon\rho}} \left[-\frac{\sigma_2}{4\sigma_1} + \frac{\sigma_2 \cdot \text{JacobiNC}\left(\frac{\sqrt{\sigma_1 k_1}}{2\sigma_1} \xi, \frac{\sqrt{k_1 k_2}}{2k_1}\right)}{4\sigma_1} \right]. \tag{43}$$

$$U_{08}(\xi) = -\frac{\sigma_2}{4\rho\epsilon\sqrt{-\frac{\sigma_1}{\epsilon\rho}}} + \sqrt{-\frac{\sigma_1}{\epsilon\rho}} \left[-\frac{\sigma_2}{4\sigma_1} + \frac{\sigma_2 \cdot \text{JacobiND}\left(\frac{\sqrt{\sigma_1 k_2}}{2\sigma_1} \xi, \frac{2\sqrt{k_1 k_2}}{k_2}\right)}{4\sigma_1} \right]. \tag{44}$$

- If $\sigma_1 > 0, k_2 < 0,$

$$U_{09}(\xi) = -\frac{\sigma_2}{4\rho\epsilon\sqrt{-\frac{\sigma_1}{\epsilon\rho}}} + \sqrt{-\frac{\sigma_1}{\epsilon\rho}} \left[-\frac{\sigma_2}{4\sigma_1} + \frac{\sigma_2 \cdot \text{JacobiNS}\left(\frac{\sigma_2}{2\sqrt{\sigma_1}} \xi, \frac{\sqrt{-k_2}}{\sigma_2}\right)}{4\sigma_1} \right]. \tag{45}$$

$$U_{10}(\xi) = -\frac{\sigma_2}{4\rho\epsilon\sqrt{-\frac{\sigma_1}{\epsilon\rho}}} + \sqrt{-\frac{\sigma_1}{\epsilon\rho}} \left[-\frac{\sigma_2}{4\sigma_1} + \frac{\sqrt{-k_2} \cdot \text{JacobiNS}\left(\frac{\sqrt{-\sigma_1 k_2}}{4\sigma_1} \xi, \frac{\sigma_2}{\sqrt{-k_2}}\right)}{4\sigma_1} \right]. \tag{46}$$

$$U_{11}(\xi) = -\frac{\sigma_2}{4\rho\epsilon\sqrt{-\frac{\sigma_1}{\epsilon\rho}}} + \sqrt{-\frac{\sigma_1}{\epsilon\rho}} \left[-\frac{\sigma_2}{4\sigma_1} + \frac{\sqrt{-k_2} \cdot \text{JacobiSN}\left(\frac{\sigma_2}{2\sqrt{\sigma_1}}\xi, \frac{\sqrt{-k_2}}{\sigma_2}\right)}{4\sigma_1} \right]. \tag{47}$$

$$U_{12}(\xi) = -\frac{\sigma_2}{4\rho\epsilon\sqrt{-\frac{\sigma_1}{\epsilon\rho}}} + \sqrt{-\frac{\sigma_1}{\epsilon\rho}} \left[-\frac{\sigma_2}{4\sigma_1} + \frac{\sigma_2 \cdot \text{JacobiSN}\left(\frac{\sqrt{-\sigma_1 k_2}}{4\sigma_1}\xi, \frac{\sigma_2}{\sqrt{-k_2}}\right)}{4\sigma_1} \right]. \tag{48}$$

Case 02: when $\sigma_4 := \frac{\sigma_2 k_1}{8\sigma_1^2}, \sigma_5 = \frac{k_1^2}{64\sigma_3^3}$ then Eq. (12) has the following hyperbolic and trigonometric solutions:

- If $\sigma_1 > 0, k_3 < 0$,

$$U_{13}(\xi) = -\frac{\sigma_2}{4\rho\epsilon\sqrt{-\frac{\sigma_1}{\epsilon\rho}}} + \sqrt{-\frac{\sigma_1}{\epsilon\rho}} \left[-\frac{\sigma_2}{4\sigma_1} + \frac{\sqrt{-k_3} \cdot \tanh\left(\frac{\sqrt{-\sigma_1 k_3}}{4\sigma_1}\right)}{4\sigma_1} \xi \right]. \tag{49}$$

$$U_{14}(\xi) = -\frac{\sigma_2}{4\rho\epsilon\sqrt{-\frac{\sigma_1}{\epsilon\rho}}} + \sqrt{-\frac{\sigma_1}{\epsilon\rho}} \left[-\frac{\sigma_2}{4\sigma_1} + \frac{\sqrt{-k_3} \cdot \coth\left(\frac{\sqrt{-\sigma_1 k_3}}{4\sigma_1}\right)}{4\sigma_1} \xi \right]. \tag{50}$$

- If $\sigma_1 > 0, k_3 > 0$,

$$U_{15}(\xi) = -\frac{\sigma_2}{4\rho\epsilon\sqrt{-\frac{\sigma_1}{\epsilon\rho}}} + \sqrt{-\frac{\sigma_1}{\epsilon\rho}} \left[-\frac{\sigma_2}{4\sigma_1} + \frac{\sqrt{k_3} \cdot \tan\left(\frac{\sqrt{\sigma_1 k_3}}{4\sigma_1}\right)}{4\sigma_1} \xi \right]. \tag{51}$$

$$U_{16}(\xi) = -\frac{\sigma_2}{4\rho\epsilon\sqrt{-\frac{\sigma_1}{\epsilon\rho}}} + \sqrt{-\frac{\sigma_1}{\epsilon\rho}} \left[-\frac{\sigma_2}{4\sigma_1} + \frac{\sqrt{k_3} \cdot \cot\left(\frac{\sqrt{\sigma_1 k_3}}{4\sigma_1}\right)}{4\sigma_1} \xi \right]. \tag{52}$$

Case 03: when $\sigma_4 := \frac{\sigma_2 k_1}{8\sigma_1^2}, \sigma_5 = \frac{\sigma_2^2 k_2}{256\sigma_3^3}$ then we get the solution Eq. (12) has the following form:

- If $\sigma_1 < 0, k_3 < 0$,

$$U_{17}(\xi) = -\frac{\sigma_2}{4\rho\epsilon\sqrt{-\frac{\sigma_1}{\epsilon\rho}}} + \sqrt{-\frac{\sigma_1}{\epsilon\rho}} \left[-\frac{\sigma_2}{4\sigma_1} + \frac{\sqrt{-2k_3} \cdot \text{sech}\left(\frac{\sqrt{2}\sqrt{\sigma_1 k_3}}{4\sigma_1}\right)}{4\sigma_1} \xi \right]. \tag{53}$$

- If $\sigma_1 > 0, k_3 > 0$,

$$U_{18}(\xi) = -\frac{\sigma_2}{4\rho\epsilon\sqrt{-\frac{\sigma_1}{\epsilon\rho}}} + \sqrt{-\frac{\sigma_1}{\epsilon\rho}} \left[-\frac{\sigma_2}{4\sigma_1} + \frac{\sqrt{2}\sqrt{k_3} \cdot \text{csch}\left(\frac{\sqrt{2}\sqrt{\sigma_1 k_3}}{4\sigma_1}\xi\right)}{4\sigma_1} \right]. \tag{54}$$

- If $\sigma_1 > 0, k_3 < 0$,

$$U_{19}(\xi) = -\frac{\sigma_2}{4\rho\epsilon\sqrt{-\frac{\sigma_1}{\epsilon\rho}}} + \sqrt{-\frac{\sigma_1}{\epsilon\rho}} \left[-\frac{\sigma_2}{4\sigma_1} + \frac{\sqrt{-2k_3} \cdot \sec\left(\frac{\sqrt{-2\sigma_1 k_3}}{4\sigma_1}\right)}{4\sigma_1} \xi \right]. \tag{55}$$

$$U_{20}(\xi) = -\frac{\sigma_2}{4\rho\epsilon\sqrt{-\frac{\sigma_1}{\epsilon\rho}}} + \sqrt{-\frac{\sigma_1}{\epsilon\rho}} \left[-\frac{\sigma_2}{4\sigma_1} + \frac{\sqrt{-2k_3} \cdot \csc\left(\frac{\sqrt{-2\sigma_1 k_3}}{4\sigma_1}\right)}{4\sigma_1} \xi \right]. \tag{56}$$

Case 04: when $\sigma_2 = \sigma_4 = \sigma_5 = 0, \sigma_3 > 0$ then we find out the solution of Eq. (12) as:

$$U_{21}(\xi) = \frac{4\sqrt{-\frac{\sigma_1}{\epsilon\rho}} \cdot \zeta \cdot \sigma_3}{4\zeta \exp(\sqrt{\sigma_3\xi}) - \sigma_1\sigma_3 \exp(-\sqrt{\sigma_3\xi})}. \quad (57)$$

The new Kudryashov method

Here are the main steps of the new Kudryashov method (NK)⁷⁷.

Step 01: The NK method provides the solution of Eq. (10) as:

$$\Phi(\xi) = c_0 + \sum_{j=1}^N (b_j f^j(\xi)). \quad (58)$$

where the coefficients b_i for $(i = 0, 1, 2, \dots, N)$ are constants to be determined such that $b_N \neq 0$, and $f(\xi) = \frac{1}{aB\sigma\xi + bB^{-\sigma\xi}}$ is the solution of the following non-linear ODE:

$$f'(\xi)^2 = (\sigma \ln(B)f(\xi))^2 (1 - 4abf^2(\xi)). \quad (59)$$

$$f''(\xi) = (\sigma^2 \ln(B)^2 f(\xi))(1 - 8abf^2(\xi)). \quad (60)$$

here constants a, b, σ , and B are all non-zero, with $B > 0$ and $B \neq 1$.

Step 02: Using the homogeneous balance principle, we may get the positive integer N by balancing the highest-order derivative and nonlinear variables in Eq. (10).

Step 03: After inserting Eq. (58) into Eq. (10) and recognizing that $f(\xi) \neq 0$ we set all coefficients of $f^i(\xi)$ to zero. After that, we get particular values for a, b , and the c_i 's by solving the resultant non-linear algebraic system. By plugging the values back into Eq. (61) and applying the transformation of Eq. (4), we may get a solution for Eq. (1).

Solutions by NK method

The exact solution of Eq. (10), by plugging value of $N=1$ in to Eq. (58) then Eq. (58) will become as follows:

$$\Phi(\xi) := b_0 + b_1 f(\xi). \quad (61)$$

By putting the value of Eq. (61) and Eq. (59,60) in Eq. (10) we obtain the following set of algebraic equations by equating the coefficients of different powers of $f(\xi)$ equal to zero. Then values of unknown constants are obtained by solving the system of algebraic equations simultaneously.

Set 01:

$$\eta = \frac{\delta(\sigma^2 \theta \ln(B)^2 + \theta n^2 - 2n)}{\sigma^2 \theta^2 \ln(B)^2 + n^2 \theta^2 - 2n\theta + 1}, \quad \theta = \theta, \quad b_0 = 0, \quad b_1 = 2\sqrt{\frac{ab}{\gamma\epsilon}} \ln(B)\sigma. \quad (62)$$

Set 02:

$$\eta = -2\delta n, \quad \theta = 0, \quad b_0 = b_0, \quad b_1 = b_1. \quad (63)$$

By inserting Set 1 in Eq. (61), we find out the solution as follows:

$$U_1(x, t) = \frac{2\sqrt{\frac{ab}{\gamma\epsilon}} \ln(B)\sigma}{aB\sigma\xi + bB^{-\sigma\xi}}. \quad (64)$$

By inserting Set 2 in Eq. (61), we find out the solution as follows:

$$U_2(x, t) = b_0 + \frac{b_1}{aB\sigma\xi + bB^{-\sigma\xi}}. \quad (65)$$

Riccati equation method

The following are the fundamental steps of the Riccati equation method (RE)⁷⁸.

Step:01 The RE method provides the solution of Eq. (10) as:

$$\Phi(\xi) = b_0 + \sum_{j=1}^N b_j f(\xi)^j. \quad (66)$$

where $f(\xi)$ satisfies the ODE, and the constants b_j for $(j = 1, 2, \dots, N)$ will be obtained subsequently such that $b_N \neq 0$ and $f(\xi)$ holds the RE.

$$f'(\xi) = \sigma_0 + \sigma_1 f(\xi) + \sigma_2 f(\xi)^2, \quad \sigma_2 \neq 0. \quad (67)$$

with σ_0, σ_1 and σ_2 are arbitrary constants. The answers to Eq. (67) are as follows.

- If $\mu > 0$, then,

$$f(\xi) = -\frac{\sigma_1}{2\sigma_2} - \frac{\sqrt{\mu}}{2\sigma_2} \tanh \left[\frac{\sqrt{\mu}}{2} \xi + \xi_0 \right]. \tag{68}$$

- If $\mu > 0$, then,

$$f(\xi) = -\frac{\sigma_1}{2\sigma_2} - \frac{\sqrt{\mu}}{2\sigma_2} \coth \left[\frac{\sqrt{\mu}}{2} \xi + \xi_0 \right]. \tag{69}$$

- If $\mu < 0$, then,

$$f(\xi) = -\frac{\sigma_1}{2\sigma_2} - \frac{\sqrt{-\mu}}{2\sigma_2} \tan \left[\frac{\sqrt{-\mu}}{2} \xi + \xi_0 \right]. \tag{70}$$

- If $\mu < 0$, then,

$$f(\xi) = -\frac{\sigma_1}{2\sigma_2} - \frac{\sqrt{-\mu}}{2\sigma_2} \cot \left[\frac{\sqrt{-\mu}}{2} \xi + \xi_0 \right]. \tag{71}$$

- If $\mu = 0$, then,

$$f(\xi) = -\frac{\sigma_1}{2\sigma_2} - \left[\frac{1}{\xi\sigma_2 + \xi_0} \right]. \tag{72}$$

Where, $\mu = \sigma_1^2 - 4\sigma_0\sigma_2$.

Step:02 By using the highest order derivative and non-linear term present in Eq. (10) and deriving the value of N with the help of the Homogeneous balance principal.

Step:03 After plugging Eqs. (66,67) in Eq. (10) and taking into account that $G(\xi) \neq 0$ we put all the constants of $f^i(\xi) = 0$. Next, we get particular values for a, b, and the b'_j s by solving the resultant non-linear algebraic system. By inserting values in Eq. (73) and utilizing transformation Eq. (4), we can get the solutions of Eq. (1).

Solution by Riccati equation method

The precise solution of Eq. (10) can find out by plugging $N = 1$ in to Eq. (66) then Eq. (66) will become as follows:

$$\Phi(\xi) = b_0 + b_1 f(\xi). \tag{73}$$

By putting the value of Eqs. (73) and (67) in Eq. (10) we obtain the following set of algebraic equations by equating the coefficients of different powers of $f(\xi)$ is equal to zero. Then values of unknown constants are obtained by solving the system of algebraic equations simultaneously.

Set 1:

$$\eta = \frac{(2n^2\theta + 4\theta\sigma_0\sigma_2 - \theta\sigma_1^2 - 4n)\delta}{2n^2\theta^2 + 4\theta^2\sigma_0\sigma_2 - \theta^2\sigma_1^2 - 4n\theta + 2}, \quad \theta = \theta, \quad b_0 = -\frac{\sigma_1}{2\epsilon\gamma\sqrt{\frac{-1}{\epsilon\gamma}}}, \quad b_1 = \sqrt{\frac{-1}{\epsilon\gamma}}\sigma_2. \tag{74}$$

Family 01: Solutions corresponding to Set 1 are given below:

Case 01.

- when $\mu > 0$ then,

$$\mathcal{U}_1(x, t) = -\frac{\sigma_1}{2\epsilon\gamma\sqrt{\frac{-1}{\epsilon\gamma}}} + \sqrt{\frac{-1}{\epsilon\gamma}}\sigma_2 \left[-\frac{\sigma_1}{2\sigma_2} - \frac{\sqrt{-4\sigma_0\sigma_2 + \sigma_1^2} \tanh \left(\frac{\sqrt{-4\sigma_0\sigma_2 + \sigma_1^2}\xi + d}{2} \right)}{2\sigma_2} \right]. \tag{75}$$

Case 02:

- when $\mu > 0$ then,

$$\mathcal{U}_2(x, t) = -\frac{\sigma_1}{2\epsilon\gamma\sqrt{\frac{-1}{\epsilon\gamma}}} + \sqrt{\frac{-1}{\epsilon\gamma}}\sigma_2 \left[-\frac{\sigma_1}{2\sigma_2} - \frac{\sqrt{-4\sigma_0\sigma_2 + \sigma_1^2} \coth\left(\frac{\sqrt{-4\sigma_0\sigma_2 + \sigma_1^2}\xi}{2} + d\right)}{2\sigma_2} \right]. \quad (76)$$

Case 03:

- when $\mu < 0$ then,

$$\mathcal{U}_3(x, t) = -\frac{\sigma_1}{2\epsilon\gamma\sqrt{\frac{-1}{\epsilon\gamma}}} + \sqrt{\frac{-1}{\epsilon\gamma}}\sigma_2 \left[-\frac{\sigma_1}{2\sigma_2} - \frac{\sqrt{4\sigma_0\sigma_2 - \sigma_1^2} \tan\left(\frac{\sqrt{4\sigma_0\sigma_2 - \sigma_1^2}\xi}{2} + d\right)}{2\sigma_2} \right]. \quad (77)$$

Case 04:

- when $\mu < 0$ then,

$$\mathcal{U}_4(x, t) = -\frac{\sigma_1}{2\epsilon\gamma\sqrt{\frac{-1}{\epsilon\gamma}}} + \sqrt{\frac{-1}{\epsilon\gamma}}\sigma_2 \left[-\frac{\sigma_1}{2\sigma_2} - \frac{\sqrt{4\sigma_0\sigma_2 - \sigma_1^2} \cot\left(\frac{\sqrt{4\sigma_0\sigma_2 - \sigma_1^2}\xi}{2} + d\right)}{2\sigma_2} \right]. \quad (78)$$

Case 05:

- when $\mu = 0$ then,

$$\mathcal{U}_5(x, t) = -\frac{\sigma_1}{2\epsilon\gamma\sqrt{\frac{-1}{\epsilon\gamma}}} + \sqrt{\frac{-1}{\epsilon\gamma}}\sigma_2 \left[-\frac{\sigma_1}{2\sigma_2} - \frac{1}{\xi\sigma_2 + d} \right]. \quad (79)$$

Graphical representation and discussion

The pictorial appearance of the solutions produced is investigated in this section. Specific values are supplied to the unknown constants to construct 3D and 2D graphs of the resulting solutions. The figures depicted in part (a) reflect a 3D plot, while part (b) represents the 2D line graph of the solutions, part (c) displays the Contour graph, and part (d) depicts the density plot. Figure 1 illustrates periodic solitary wave with varying values of constants $\mathcal{U}_{01}(x, t)$: $\sigma_1 = -2, \sigma_2 = 1, \sigma_3 = -1, k_1 = 7, n = 1, \eta = 1, \theta = 0.3, \epsilon = 4, \rho = 0.01, \delta = 0.78, \xi = x - \eta t$, for line graph $t = -1, 0, 1$. Figure 2 represents dark solitary wave with varying values of constants $\mathcal{U}_{02}(x, t)$: $\sigma_1 = -0.2, \sigma_2 = 0.8, \sigma_3 = -1, k_1 = 0.16, n = 1, \eta = 2, \theta = 0.3, \epsilon = 5, \rho = 2, \delta = 1.44, \xi = x - \eta t$, for line graph $t = -1, 0, 1$. Figure 3 represents periodic solitary wave with $\mathcal{U}_{03}(x, t)$: $\sigma_1 = -0.1, \sigma_2 = 0.6, \sigma_3 = 0.1, k_1 = -0.40, k_2 = -1.96, n = -1, \eta = 2, \theta = 0.3, \epsilon = 5, \rho = 2, \delta = 1.33, \xi = x - \eta t$, for line graph $t = -1, 0, 1$. Figure 4 represents periodic solitary wave with varying values of constants $\mathcal{U}_{04}(x, t)$: $\sigma_1 = -0.1, \sigma_2 = 0.4, \sigma_3 = 0.1, k_1 = -0.20, k_2 = -0.96, n = -1, \eta = 1, \theta = 0.3, \epsilon = 5, \rho = 2, \delta = 0.69, \xi = x - \eta t$, for line graph $t = -1, 0, 1$. Figure 5 represents bright solitary wave with different values of constants $\mathcal{U}_{05}(x, t)$: $\sigma_1 = -0.2, \sigma_2 = 0.28, \sigma_3 = -0.1, k_1 = -0.0016, k_2 = -0.0720, n = -1, \eta = 0.5, \theta = 0.3, \epsilon = 2, \rho = 0.36, \delta = 0.69, \xi = x - \eta t$, for line graph $t = -1, 0, 1$. Figure 6 indicates kink solitary wave with specific values of constants $\mathcal{U}_{13}(x, t)$: $\sigma_1 = 0.2, \sigma_2 = -0.4, \sigma_3 = 0.1, k_3 = -0.32, n = -2, \eta = -1, \theta = 0.3, \epsilon = -2, \rho = 1, \delta = 0.49, \xi = x - \eta t$, for line graph $t = -1, 0, 1$. Figure 7 indicates dark solitary wave with $\mathcal{U}_{15}(x, t)$: $\sigma_1 = 0.01, \sigma_2 = 0.02, \sigma_3 = 0.03, k_3 = -0.0012, n = -2, \eta = 0.2, \theta = 0.3, \epsilon = 4, \rho = 0.2, \delta = 0.09, \xi = x - \eta t$, for line graph $t = -1, 0, 1$. Figure 8 depicts dark solitary wave with $\mathcal{U}_{17}(x, t)$: $\sigma_1 = -0.02, \sigma_2 = 0.03, \sigma_3 = 0.04, k_3 = -0.91, n = 1, \eta = 6.5, \theta = 3, \epsilon = 2, \rho = 2, \delta = 21.90, \xi = x - \eta t$, for line graph $t = -1, 0, 1$. Figure 9 depicts bright solitary wave with varying values of constants $\mathcal{U}_1(x, t)$: $a = 1, b = 3, B = 0.5, \sigma = -1, \gamma = 1, \theta = 0.4, \delta = 1.5, n = 0.5, \epsilon = 1, \xi = x - \eta t$, for line graph $t = -1, 0, 1$. Figure 10 represents dark solitary wave with $\mathcal{U}_2(x, t)$: $a = 1, b = 1, B = 0.5, \sigma = 1, \gamma = 1, \theta = 0.01, \delta = -1.5, n = 0.5, \epsilon = 1, b_0 = 1, b_1, \eta = 1.5, \xi = x - \eta t$, for line graph $t = -1, 0, 1$. Figure 11 indicates kink solitary wave with varying values of constants $\mathcal{U}_1(x, t)$: $\delta = -1, \sigma_0 = -1, \sigma_1 = 0.5, \sigma_2 = 0.5, \gamma = -1, n = 0.5, m = 1.5, \theta = 0.1, \eta = 1.2, d = 0.4, \epsilon = 1, \mu = 2.2, \xi = x - \eta t$, for line graph $t = -1, 0, 1$. Figure 12 indicates singular bright solitary wave with $\mathcal{U}_2(x, t)$: $\sigma_0 = -0.1, \delta = 0.3, \sigma_1 = 0.5, \gamma = -0.1, \sigma_2 = 0.2, n = 0.01, m = 0.01, \theta = 0.01, \eta = -0.006, d = 1, \epsilon = -0.1, \mu = 0.33, \xi = x - \eta t$, for line graph $t = -1, 0, 1$. Figure 13 represents singular kink solitary wave with varying values of constants $\mathcal{U}_3(x, t)$: $\sigma_0 = 0.2, \delta = 0.3, \sigma_1 = 0.01, \gamma = -1.5, \sigma_2 = 0.2, n = 0.01, m = 0.01, \theta = -0.006, d = 0.9, \epsilon = 0.01, \mu = -0.159, \xi = x - \eta t$, for line graph $t = -1, 0, 1$. Figure 14 indicates singular kink solitary wave with varying values of constants $\mathcal{U}_4(x, t)$: $\sigma_0 = 0.2, \delta = 0.3, \sigma_1 = 0.01, \gamma = -1.5, \sigma_2 = 0.2, n = 0.01, m = 0.01, \theta = 0.01, \eta = -0.006, d = 1, \epsilon = 0.01, \mu = -0.159, \xi = x - \eta t$, for line graph $t = -1, 0, 1$.

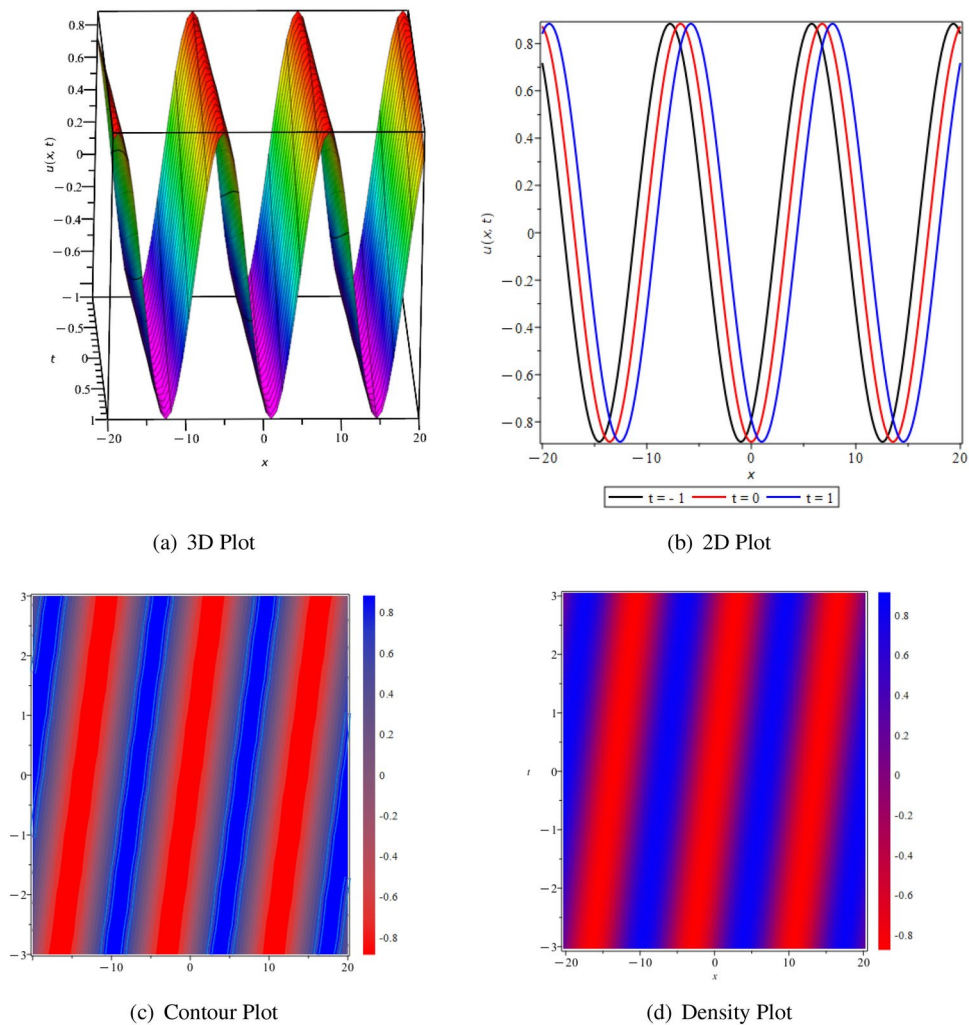


Figure 1. The visual representation of the obtained solution of Eq. (37) represented as $U_{01}(x, t) : \sigma_1 = -2, \sigma_2 = 1, \sigma_3 = -1, k_1 = 7, n = 1, \eta = 1, \theta = 0.3, \epsilon = 4, \rho = 0.01, \delta = 0.78$.

Conclusion

This work used the Kumar-Malik method, and the new Kudryashov and Riccati equation approaches to get precise solutions for the AE, a Heisenberg ferromagnet equation. AE is an essential instrument for examining nonlinear manifestation in optics, magnetism, and the differential geometry of curves and surfaces. It is often used to depict optical solitons in nonlinear optical fibers, which are essential for fiber-optic communication because of their ability to preserve shape over long distances. To achieve this purpose, it was crucial to use a particular wave transformation technique to turn the original NLPDEs into a NODEs. Notably, these approaches provided a wide range of soliton solutions, spanning periodic, bright, dark, Kink, trigonometric, rational, and exponential solitons. For a thorough comprehension of the physical processes inherent in the integrable AE, we graphically portrayed chosen solutions by assigning parameter values in 3D-surface graphs, 2D-line graphs, and contour and density plots, according to particular limitations. These graphical representations aid in deepening our knowledge of the various soliton structures originating from the equation. Additionally, we underlined the usefulness and potency of the Kumar-Malik method, and new Kudryashov, and Riccati equation strategies in discovering soliton solutions for NLPDEs. The discovered solutions contribute greatly to expanding our grasp of the nonlinear dynamics regulating the propagation of photonic solitons. This paper tries to give helpful insights for scientists and researchers aiming to enhance their experimental activities. Moreover, there exists a possibility for widening the extent of our work include issues related to lump interactions, researching multi-soliton situations, and analyzing the dynamics of rouge wave breathers. Such additions might improve the practical application and relevance of the research.

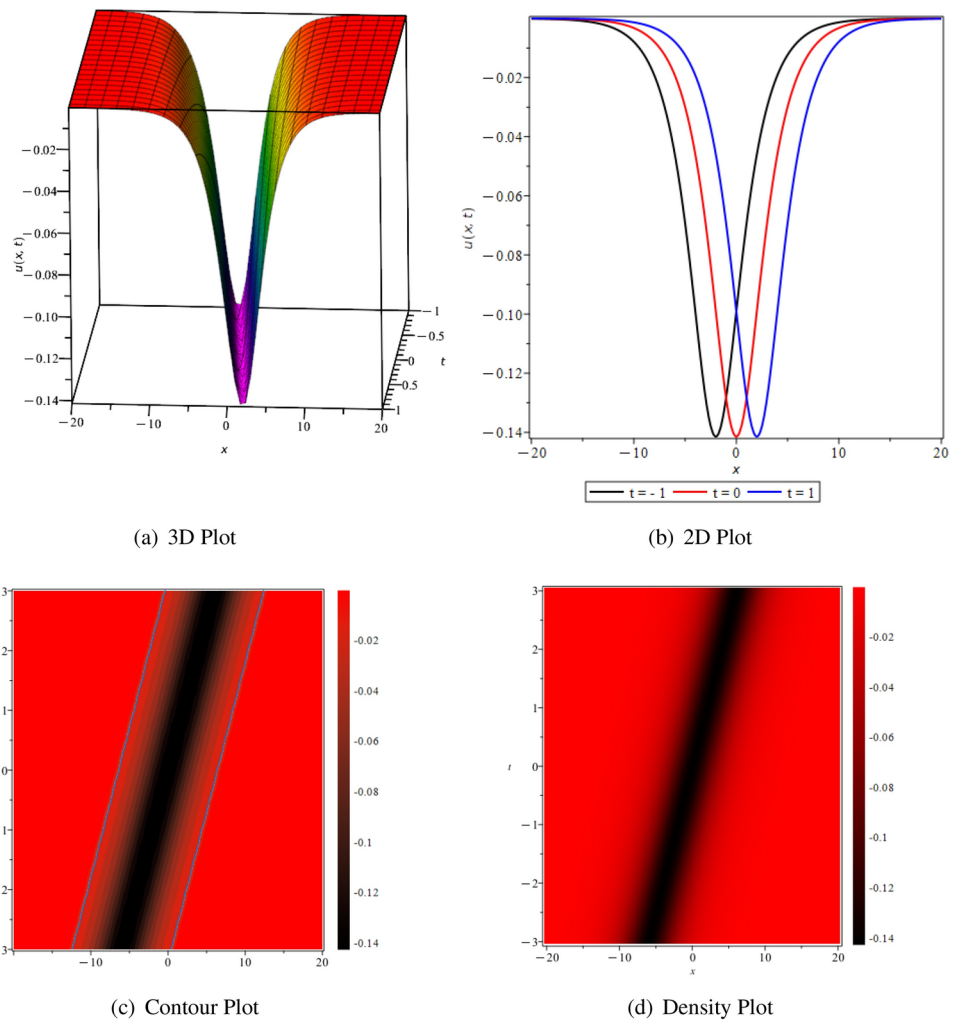


Figure 2. The visual representation of the obtained solution of Eq. (38) represented as $\mathcal{U}_{02}(x, t) : \sigma_1 = -0.2, \sigma_2 = 0.8, \sigma_3 = -1, k_1 = 0.16, n = 1, \eta = 2, \theta = 0.3, \epsilon = 5, \rho = 2, \delta = 1.44.$

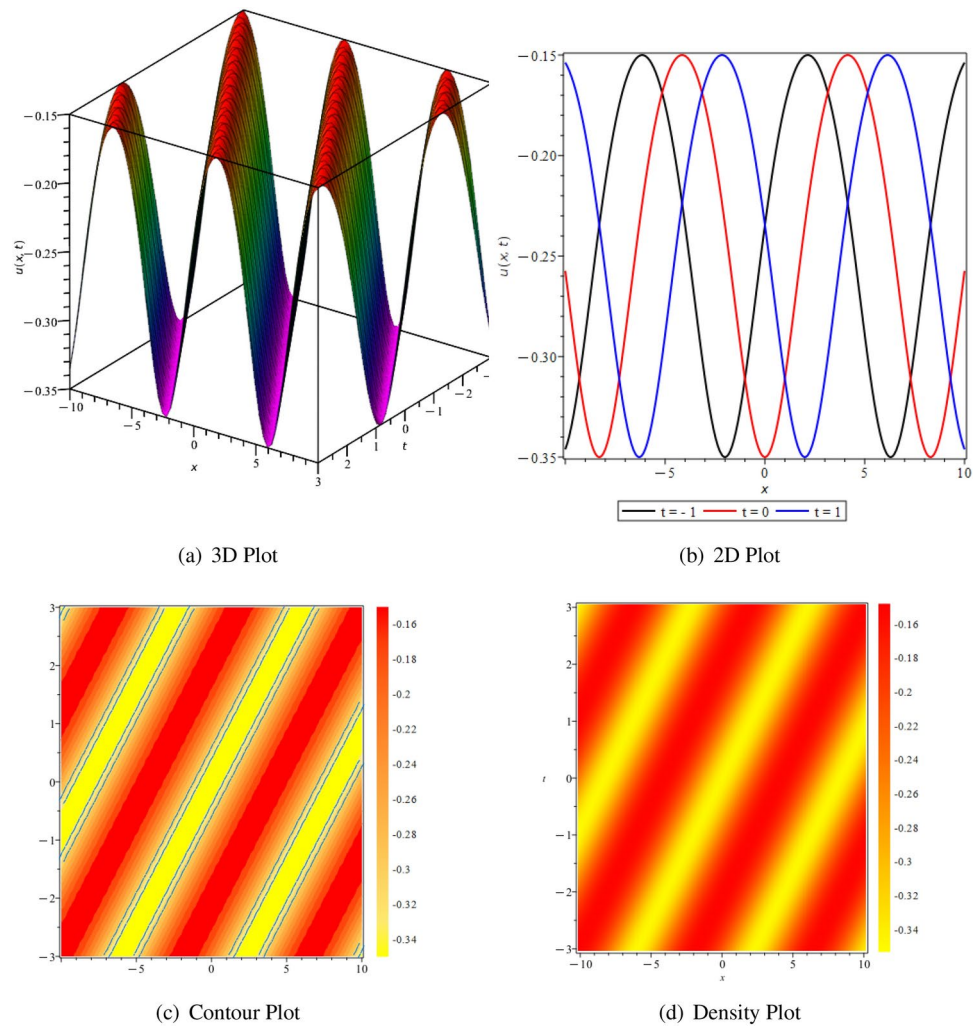


Figure 3. The visual representation of the obtained solution of Eq. (39) represented as $\mathcal{U}_{03}(x, t)$: $\sigma_1 = -0.1$, $\sigma_2 = 0.6$, $\sigma_3 = 0.1$, $k_1 = -0.40$, $k_2 = -1.96$, $n = -1$, $\eta = 2$, $\theta = 0.3$, $\epsilon = 5$, $\rho = 2$, $\delta = 1.33$.

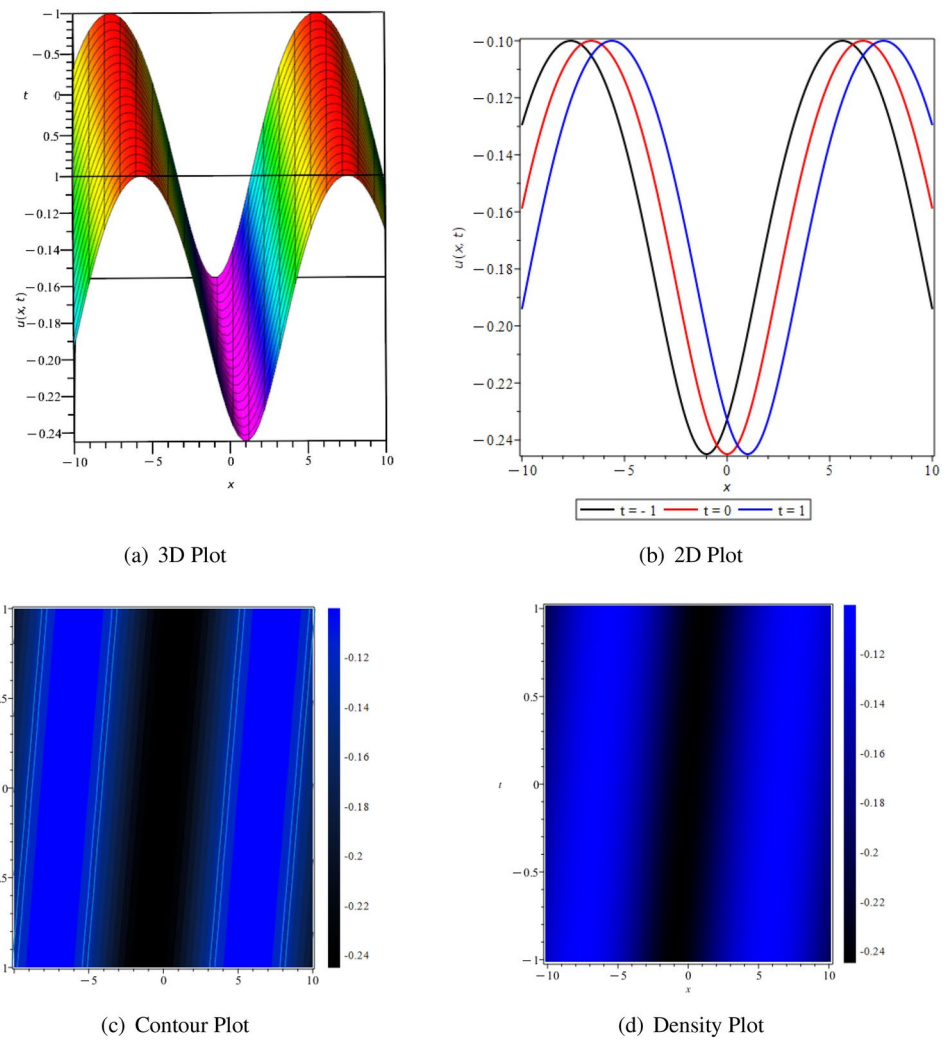
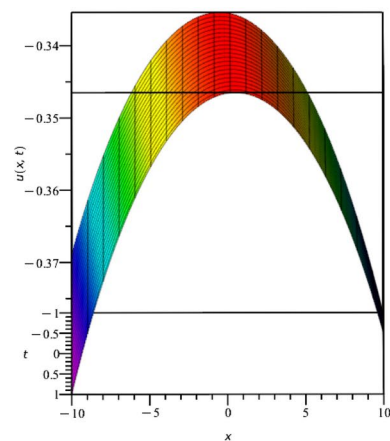
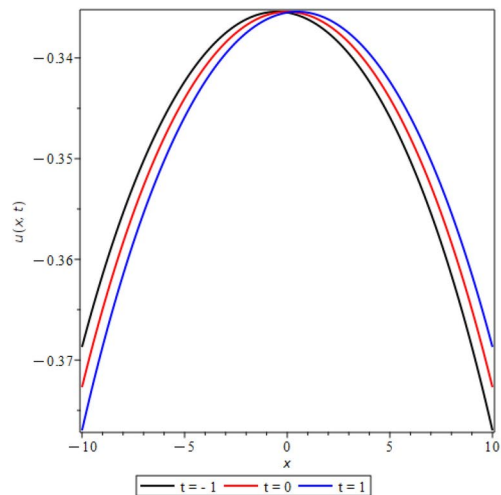


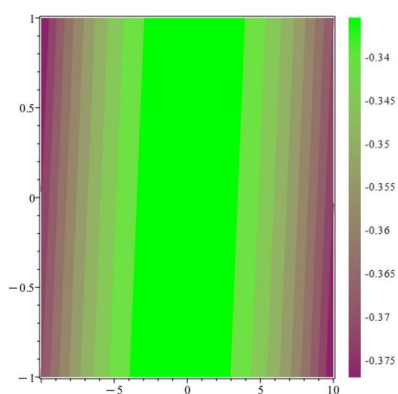
Figure 4. The visual representation of the obtained solution of Eq. (40) represented as $\mathcal{U}_{04}(x, t) : \sigma_1 = -0.1, \sigma_2 = 0.4, \sigma_3 = 0.1, k_1 = -0.20, k_2 = -0.96, n = -1, \eta = 1, \theta = 0.3, \epsilon = 5, \rho = 2, \delta = 0.69$.



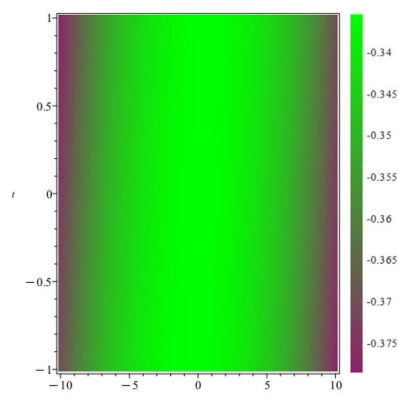
(a) 3D Plot



(b) 2D Plot



(c) Contour Plot



(d) Density Plot

Figure 5. The visual representation of the obtained solution of Eq. (41) represented as $U_{05}(x, t) : \sigma_1 = -0.2, \sigma_2 = 0.28, \sigma_3 = -0.1, k_1 = 1.006, k_2 = -0.0720, n = -1, \eta = 0.5, \theta = 0.3, \epsilon = 2, \rho = 0.36, \delta = 0.69$.

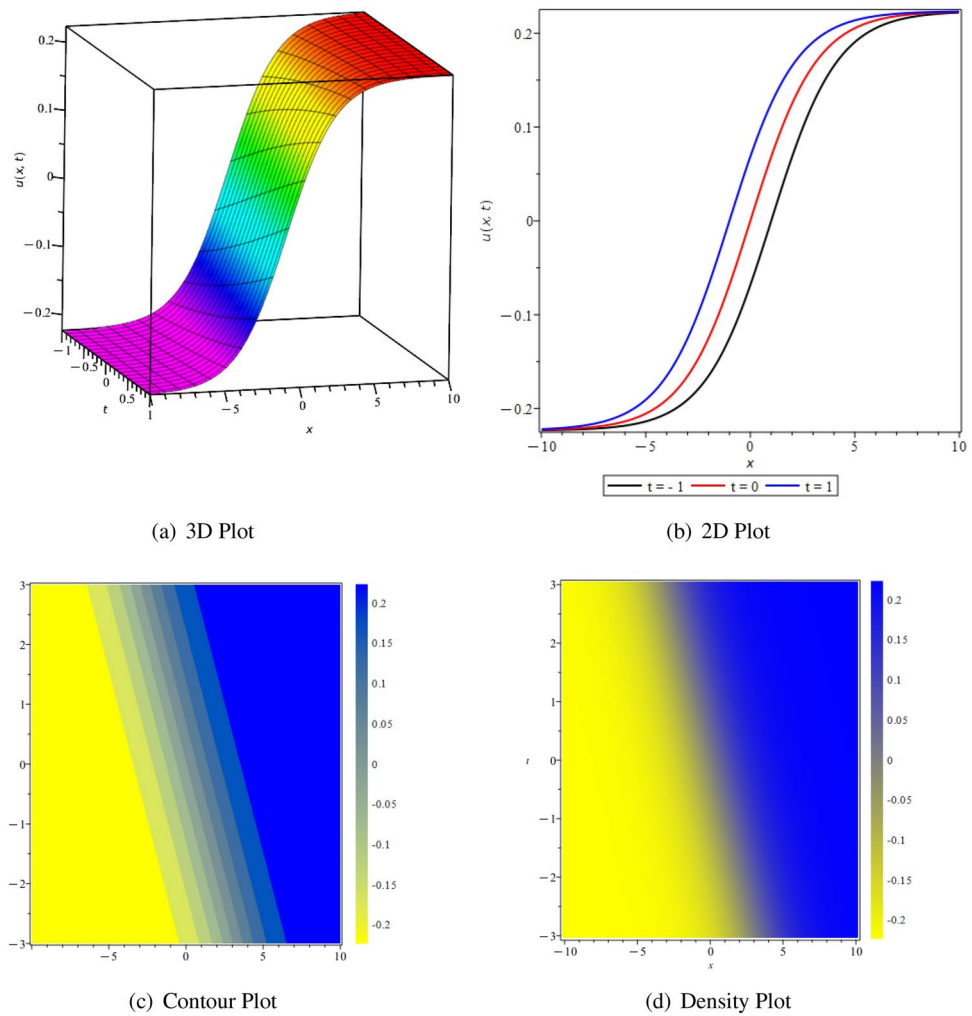
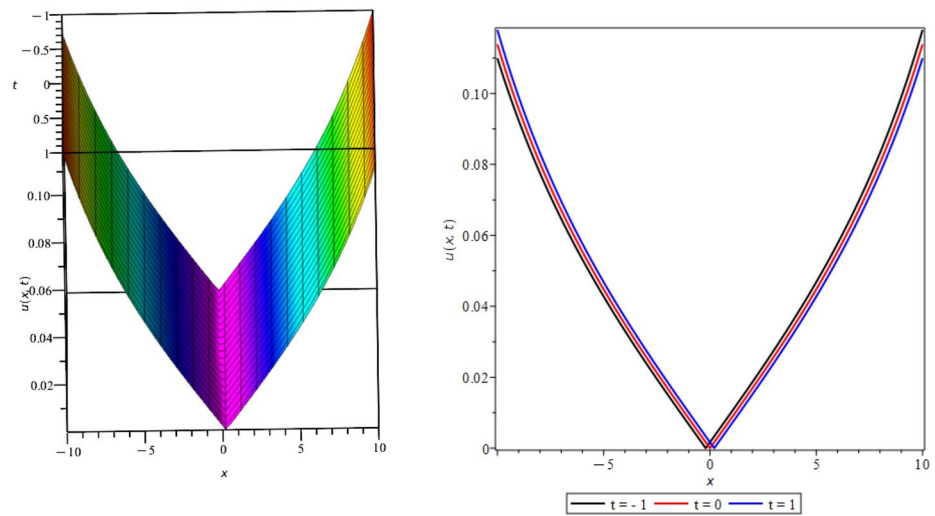
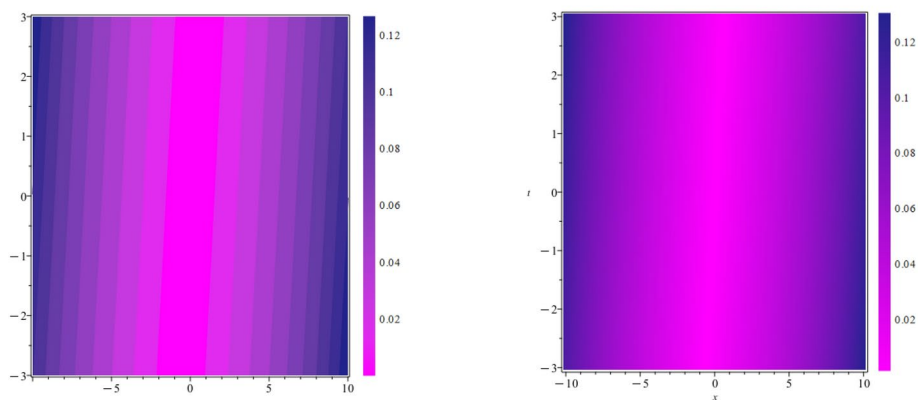


Figure 6. The visual representation of the obtained solution of Eq. (49) represented as $\mathcal{U}_{13}(x, t) : \sigma_1 = 0.2, \sigma_2 = -0.4, \sigma_3 = 0.1, k_3 = -0.32, n = -2, \eta = -1, \theta = 0.3, \epsilon = -2, \rho = 1, \delta = 0.49$.



(a) 3D Plot

(b) 2D Plot



(c) Contour Plot

(d) Density Plot

Figure 7. The visual representation of the obtained solution of Eq. (51) represented as $\mathcal{U}_{15}(x, t) : \sigma_1 = 0.01, \sigma_2 = 0.02, \sigma_3 = 0.03, k_3 = 0.0012, n = -2, \eta = 0.2, \theta = 0.3, \epsilon = 4, \rho = 0.2, \delta = 0.09$.

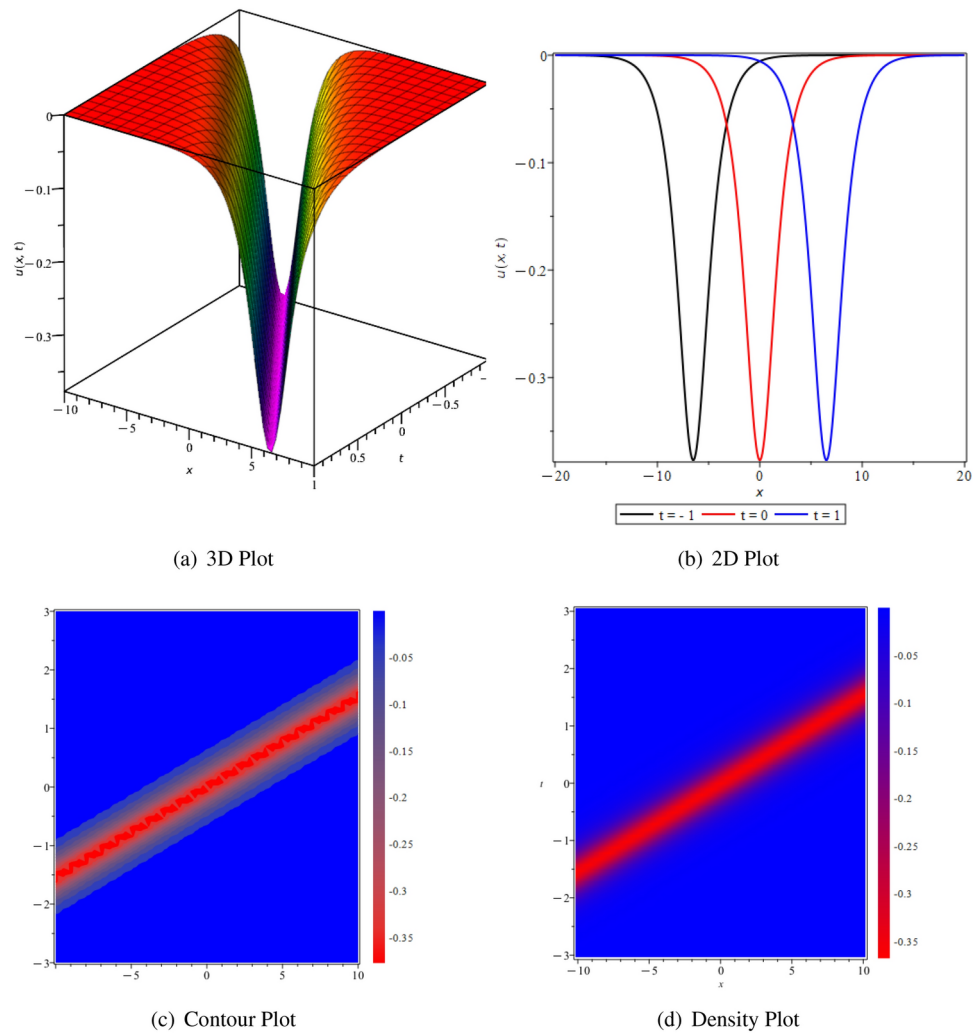
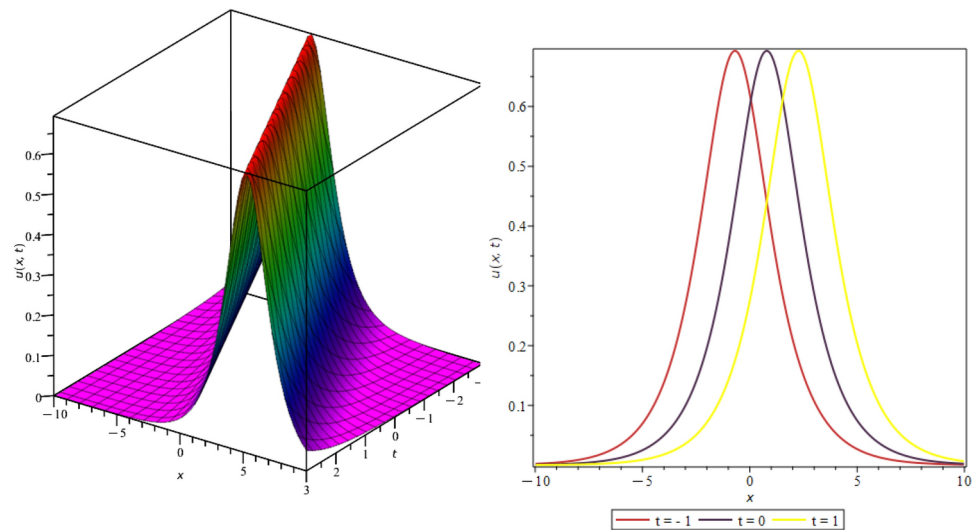
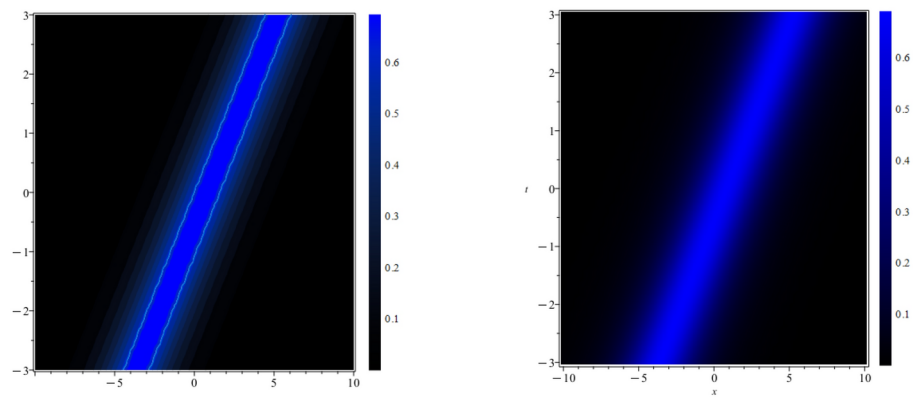


Figure 8. The visual representation of the obtained solution of Eq. (53) represented as $\mathcal{U}_{17}(x, t)$: $\sigma_1 = -0.02, \sigma_2 = 0.03, \sigma_3 = 0.04, k_3 = -0.91, n = 1, \eta = 6.5, \theta = 3, \epsilon = 2, \rho = 2, \delta = 21.90$.



(a) 3D Plot

(b) 2D Plot



(c) Contour Plot

(d) Density Plot

Figure 9. The visual representation of the obtained solution of Eq. (64) represented as $\mathcal{U}_1(x, t) : a = 1, b = 3, B = 0.5, \sigma = -1, \gamma = 1, \theta = 0.4, \delta = 1.5, n = 0.5, \epsilon = 1$.

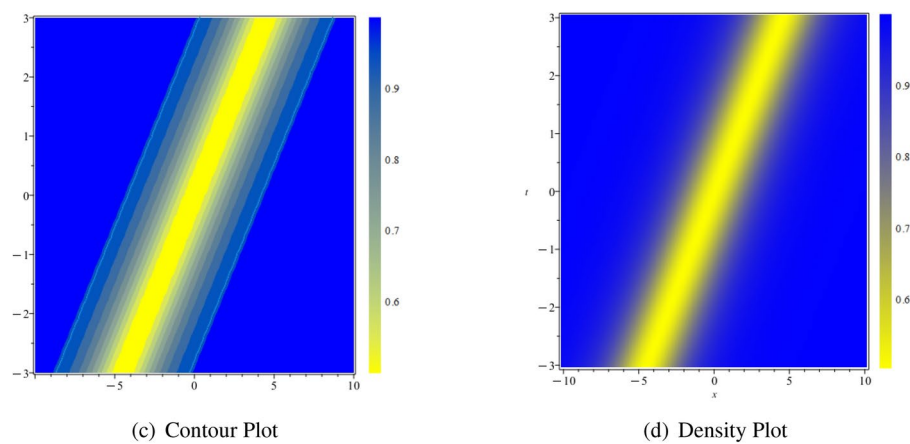
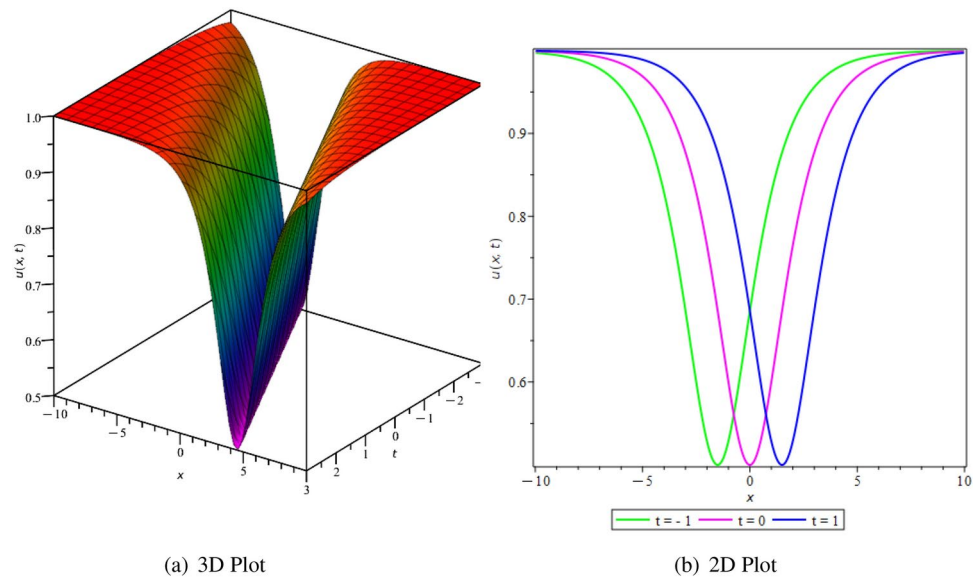


Figure 10. The visual representation of the obtained solution of Eq. (65) represented as $\mathcal{U}_2(x, t) : a = 1, b = 1, B = 0.5, \sigma = 1, \gamma = 1, \theta = 0.01, \delta = -1.5, n = 0.5, \epsilon = 1, b_0 = 1, b_1, \eta = 1.5$.

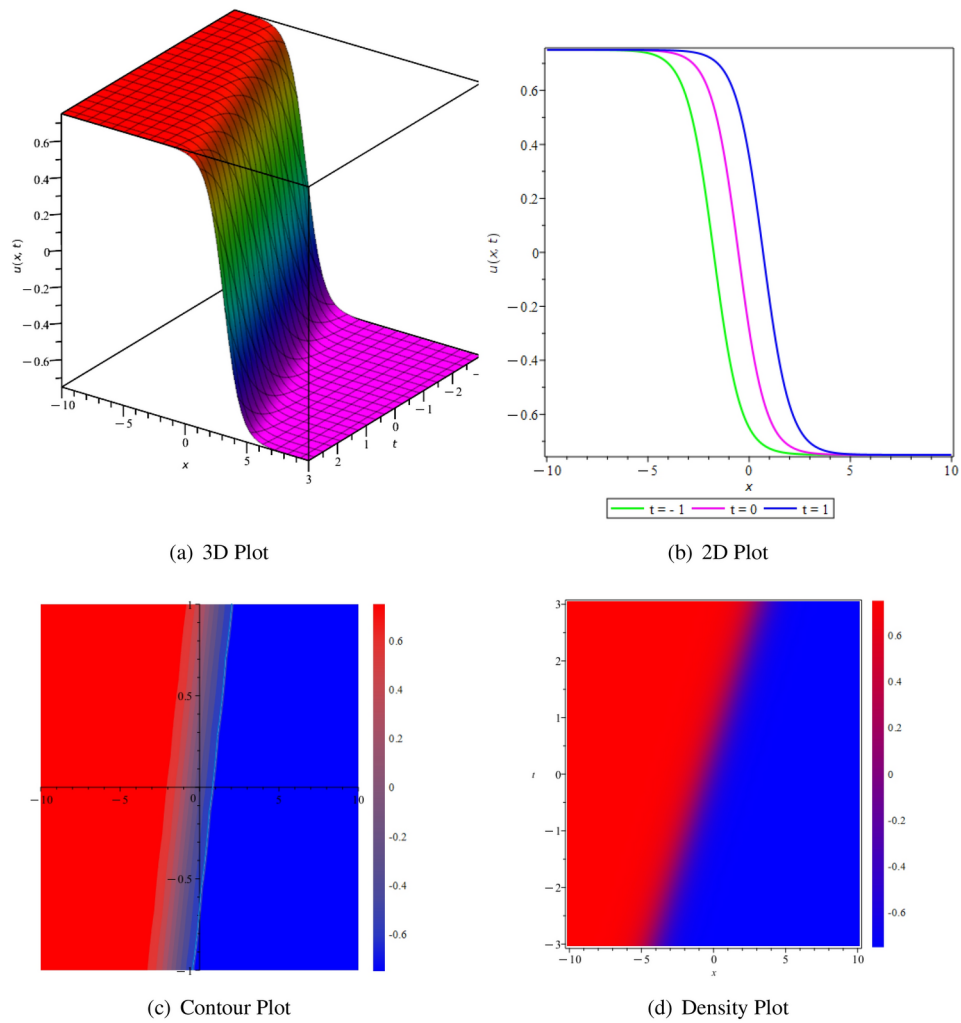


Figure 11. The visual representation of the obtained solution of Eq. (75) represented as $U_1(x, t)$: $\sigma_0 = -1, \delta = -1, \sigma_1 = 0.5, \gamma = -1, \sigma_2 = 0.5, n = 0.5, m = 1.5, \theta = 0.1, \eta = 1.2, d = 0.4, \epsilon = 1, \mu = 2.25$.

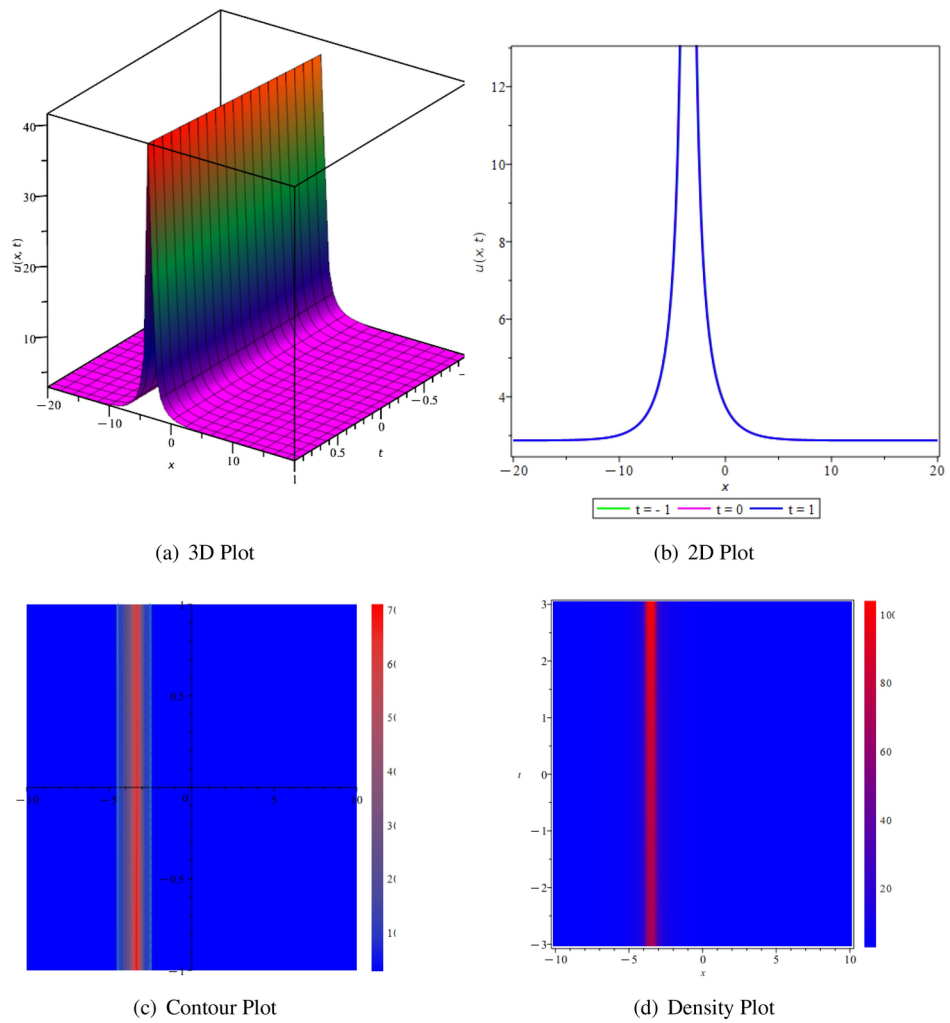


Figure 12. The visual representation of the obtained solution of Eq. (76) represented as $\mathcal{U}_2(x, t) : \sigma_0 = -0.1, \delta = 0.3, \sigma_1 = 0.5, \gamma = -0.1, \sigma_2 = 0.2, n = 0.01, m = 0.01, \theta = 0.01, \eta = -0.006, d = 1, \epsilon = -0.1, \mu = 0.33$.

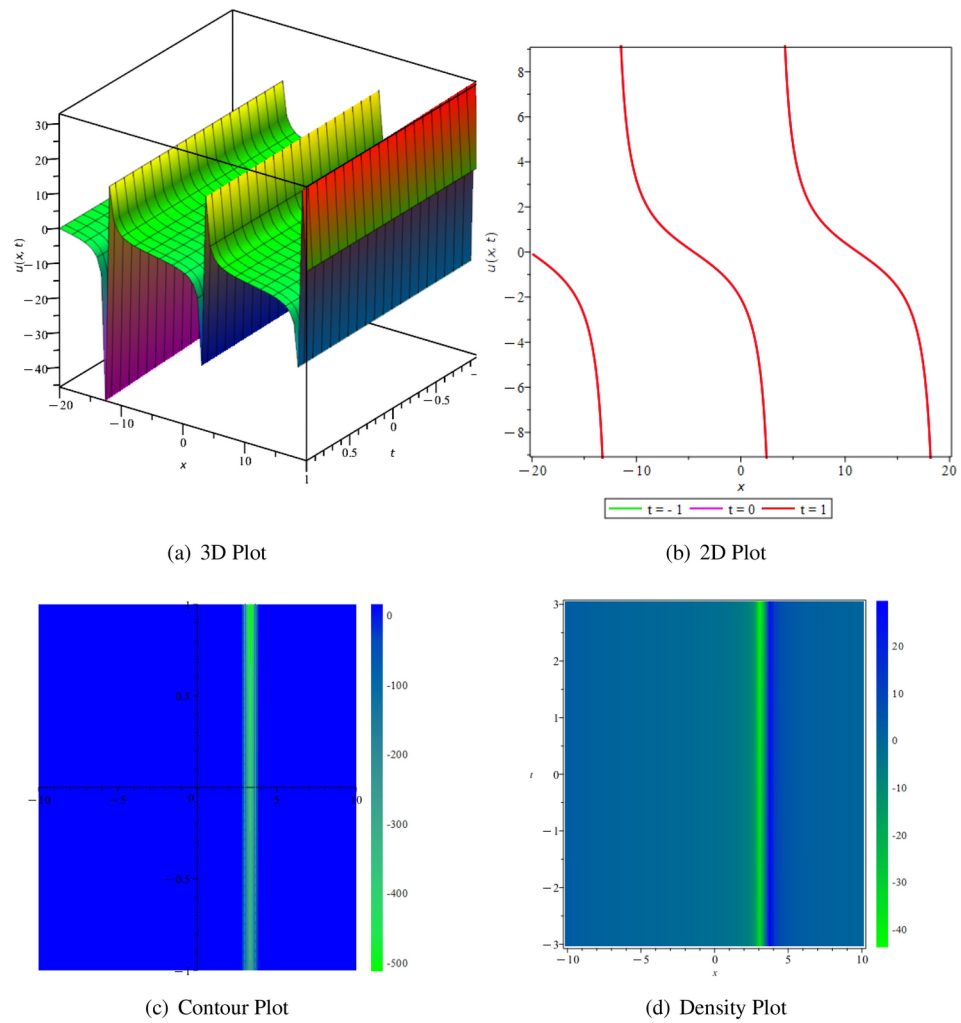


Figure 13. The visual representation of the obtained solution of Eq. (77) represented as $\mathcal{U}_3(x, t) : \sigma_0 = 0.2, \delta = 0.3, \sigma_1 = 0.01, \gamma = -1.5, \sigma_2 = 0.2, n = 0.01, m = 0.01, \theta = 0.01, \eta = -0.006, d = 0.9, \epsilon = 0.01, \mu = -0.159$.

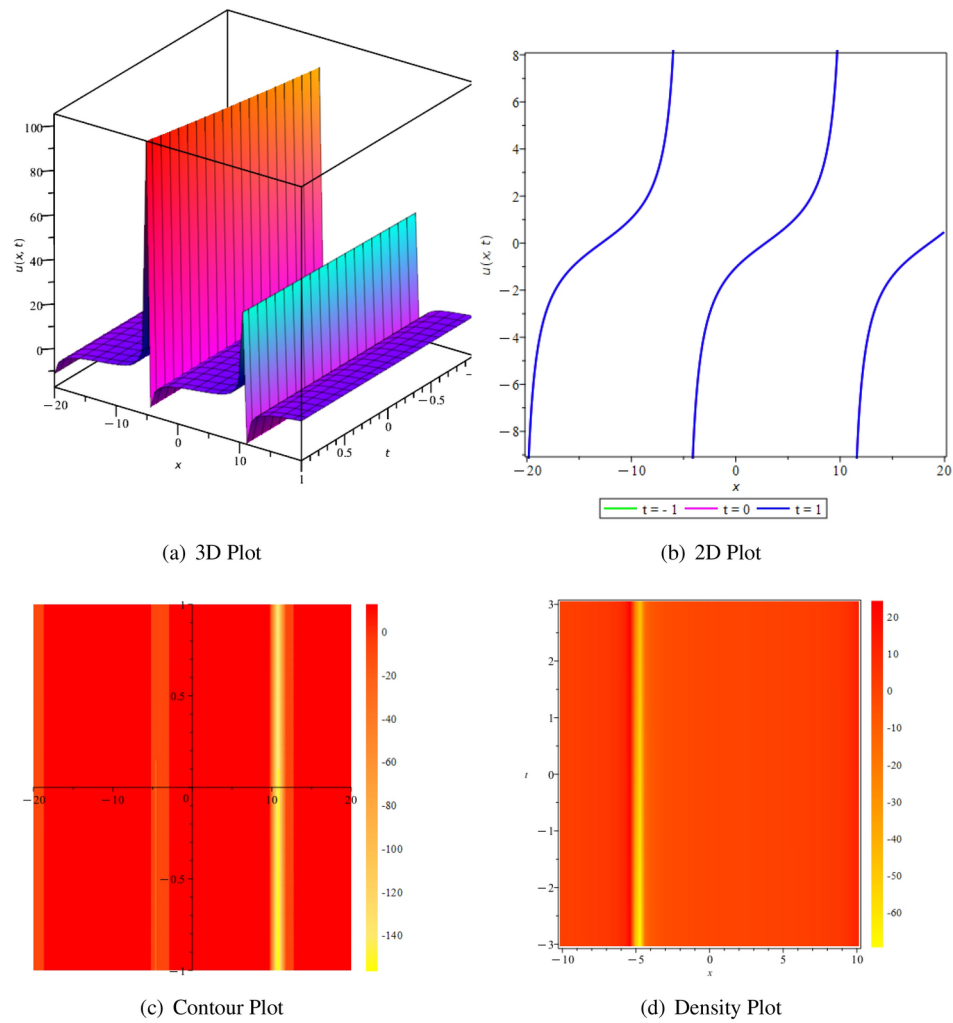


Figure 14. The visual representation of the obtained solution of Eq. (78) represented as $\mathcal{U}_4(x, t)$: $\sigma_0 = 0.2, \delta = 0.3, \sigma_1 = 0.01, \sigma_2 = 0.2, \gamma = -1.5, \sigma_2 = 0.2, n = 0.01, m = 0.01, \theta = 0.01, \eta = -0.006, d = 1, \epsilon = 0.01, \mu = -0.159$.

Data availability

The data that support the findings of this study are available from the corresponding author upon reasonable request.

Received: 23 August 2024; Accepted: 25 December 2024

Published online: 04 April 2025

References

- Islam, S. R., Khan, K. & Akbar, M. A. Optical soliton solutions, bifurcation, and stability analysis of the Chen-Lee-Liu model. *Results Phys.* **51**, 106620 (2023).
- Khater, M. M. Novel computational simulation of the propagation of pulses in optical fibers regarding the dispersion effect. *Int. J. Mod. Phys. B* **37**(09), 2350083 (2023).
- Bialynicki-Birula, I. & Mycielski, J. Nonlinear wave mechanics. *Ann. Phys.* **100**(1–2), 62–93 (1976).
- Khater, M. M. Physics of crystal lattices and plasma; Analytical and numerical simulations of the Gilson-Pickering equation. *Results Phys.* **44**, 106193 (2023).
- Ames, W. F. *Nonlinear Partial Differential Equations in Engineering* (Academic press, 1965).
- Stuart, J. T. On the non-linear mechanics of hydrodynamic stability. *J. Fluid Mech.* **4**(1), 1–21 (1958).
- Ozdemir, N., Secer, A., Ozisik, M. & Bayram, M. Optical solitons for the dispersive Schrödinger–Hirota equation in the presence of spatiotemporal dispersion with parabolic law. *Eur. Phys. J. Plus* **138**(6), 1–10 (2023).
- Rabie, W. B., Ahmed, H. M., Mirzazadeh, M., Akbulut, A. & Hashemi, M. S. Investigation of solitons and conservation laws in an inhomogeneous optical fiber through a generalized derivative nonlinear Schrödinger equation with quintic nonlinearity. *Opt. Quantum Electron.* **55**(9), 825 (2023).
- Khater, M. M. Abundant and accurate computational wave structures of the nonlinear fractional biological population model. *Int. J. Mod. Phys. B* **37**(18), 2350176 (2023).
- Attia, R. A., Xia, Y., Zhang, X. & Khater, M. M. Analytical and numerical investigation of soliton wave solutions in the fifth-order KdV equation within the KdV-kP framework. *Results Phys.* **51**, 106646 (2023).
- Akbar, M. A., Abdullah, F. A., Islam, M. T., Sharif, Mohammed A. Al. & Osman, M. S. New solutions of the soliton type of shallow water waves and superconductivity models. *Results Phys.* **44**, 106180 (2023).
- Shyaman, V. P., Sreelakshmi, A. & Awasthi, A. An adaptive tailored finite point method for the generalized Burgers' equations. *J. Comput. Sci.* **62**, 101744 (2022).
- Alharbi, R., Alshaery, A. A., Bakodah, H. O., Nuruddeen, R. I. & Gómez-Aguilar, J. F. Revisiting $(2+ 1)$ -dimensional burgers' dynamical equations: Analytical approach and Reynolds number examination. *Phys. Scr.* **98**(8), 085225 (2023).
- Skippi, J., Laurie, J. & Nazarenko, S. Hamiltonian derivation of the point vortex model from the two-dimensional nonlinear Schrödinger equation. *Phys. Rev. E* **107**(2), 025107 (2023).
- Wang, K. J. & Liu, J. H. Diverse optical solitons to the nonlinear Schrödinger equation via two novel techniques. *Eur. Phys. J. Plus* **138**(1), 1–9 (2023).
- Rizvi, S. T. R., Seadawy, A. R., Ahmed, S. & Bashir, A. Optical soliton solutions and various breathers lump interaction solutions with periodic wave for nonlinear Schrödinger equation with quadratic nonlinear susceptibility. *Opt. Quantum Electron.* **55**(3), 286 (2023).
- Akinyemi, L., Şenol, M. & Osman, M. S. Analytical and approximate solutions of nonlinear Schrödinger equation with higher dimension in the anomalous dispersion regime. *J. Ocean Eng. Sci.* **7**(2), 143–154 (2022).
- Zabihi, A. et al. Solitons solutions to the high-order dispersive cubic-quintic Schrödinger equation in optical fibers. *J. Nonlinear Opt. Phys. Mater.* **32**(03), 2350027 (2023).
- Iqbal, M. d. A., Wang, Y., Miah, M. d. M. & Osman, M. S. Study on Date-Jimbo-Kashiwara-Miwa equation with conformable derivative dependent on time parameter to find the exact dynamic wave solutions. *Fract. Fract.* **6**(1), 4 (2021).
- Eidinejad, Z., Saadati, R., Li, C., Inc, M. & Vahidi, J. The multiple exp-function method to obtain soliton solutions of the conformable Date-Jimbo-Kashiwara-Miwa equations. *Int. J. Mod. Phys. B* **38**(03), 2450043 (2024).
- Singh, S. & Ray, S. S. Integrability and new periodic, kink-antikink and complex optical soliton solutions of $(3+ 1)$ -dimensional variable coefficient Djk equation for the propagation of nonlinear dispersive waves in inhomogeneous media. *Chaos Solit. Fract.* **168**, 113184 (2023).
- Khater, M. M. A. Computational simulations of propagation of a tsunami wave across the ocean. *Chaos Solit. Fract.* **174**, 113806 (2023).
- Khater, M. M. A. Characterizing shallow water waves in channels with variable width and depth; Computational and numerical simulations. *Chaos Solit. Fract.* **173**, 113652 (2023).
- Chu, Y. M., Arshed, S., Sadaf, M., Akram, G. & Maqbool, M. Solitary wave dynamics of thin-film ferroelectric material equation. *Results Phys.* **45**, 106201 (2023).
- Zahran, E. H., Mirhosseini-Alizamini, S. M., Shehata, M. S. M., Rezazadeh, H. & Ahmad, H. Study on abundant explicit wave solutions of the thin-film ferro-electric materials equation. *Opt. Quantum Electron.* **54**(1), 48 (2022).
- Alotaibi, T. & Althobaiti, A. Exact solutions of the nonlinear modified Benjamin-Bona-Mahony equation by an analytical method. *Fract. Fract.* **6**(7), 399 (2022).
- Kutluay, S., Özer, S. & Yağmurlu, Nuri Murat. A new highly accurate numerical scheme for Benjamin-Bona-Mahony-Burgers equation describing small amplitude long wave propagation. *Mediterr. J. Math.* **20**(3), 173 (2023).
- Wang, K. Variational principle and diverse wave structures of the modified Benjamin-Bona-Mahony equation arising in the optical illusions field. *Axioms* **11**(9), 445 (2022).
- Barletta, A. The Boussinesq approximation for buoyant flows. *Mech. Res. Commun.* **124**, 103939 (2022).
- Khaliq, S., Ullah, A., Ahmad, S., Akgül, A., Yusuf, A. & Sulaiman, T. A. Some novel analytical solutions of a new extended $(2+ 1)$ -dimensional Boussinesq equation using a novel method. *J. Ocean Eng. Sci.* (2022).
- Charlier, C. & Lenells, J. On Boussinesq's equation for water waves. arXiv preprint [arXiv:2204.02365](https://arxiv.org/abs/2204.02365) (2022).
- Pu, X. & Zhou, W. The hydrostatic approximation of the Boussinesq equations with rotation in a thin domain. arXiv preprint [arXiv:2203.11418](https://arxiv.org/abs/2203.11418) (2022).
- Al Alwan, B. et al. The propagating exact solitary waves formation of generalized Calogero-Bogoyavlenskii-Schiff equation with robust computational approaches. *Fract. Fract.* **7**(2), 191 (2023).
- Zhou, Y., Zhang, X., Zhang, C., Jia, J. & Ma, W. New lump solutions to a $(3+ 1)$ -dimensional generalized Calogero-Bogoyavlenskii-Schiff equation. *Appl. Math. Lett.* **141**, 108598 (2023).
- Ul, I., Haq, N., Ali, S. Ahmad, & Akram, T. A hybrid interpolation method for fractional PDEs and its applications to fractional diffusion and buckmaster equations. *Math. Probl. Eng.* **2022**(1), 2517602 (2022).
- Faridi, W. A. & AlQahtani, S. A. The explicit power series solution formation and computation of lie point infinitesimals generators: Lie symmetry approach. *Phys. Scr.* **98**(12), 125249 (2023).
- Islam, Md. T., Akbar, Md. A., Gómez-Aguilar, J. F., Bonyah, E. & Fernandez-Anaya, G. Assorted soliton structures of solutions for fractional nonlinear Schrodinger types evolution equations. *J. Ocean Eng. Sci.* **7**(6), 528–535 (2022).

38. Islam, Md. T., Sarkar, T. R., Abdullah, F. A. & Gómez-Aguilar, J. F. Characteristics of dynamic waves in incompressible fluid regarding nonlinear Boiti-Leon-Manna-Pempinelli model. *Phys. Scr.* **98**(8), 085230 (2023).
39. Islam, Md. T., Ryehan, S., Abdullah, F. A. & Gómez-Aguilar, J. F. The effect of Brownian motion and noise strength on solutions of stochastic Bogoyavlenskii model alongside conformable fractional derivative. *Optik* **287**, 171140 (2023).
40. Qureshi, Z. A. et al. Mathematical analysis about influence of Lorentz force and interfacial nano layers on nanofluids flow through orthogonal porous surfaces with injection of swcnts. *Alex. Eng. J.* **61**(12), 12925–12941 (2022).
41. Shah, I. A. et al. On analysis of magnetized viscous fluid flow in permeable channel with single wall carbon nano tubes dispersion by executing nano-layer approach. *Alex. Eng. J.* **61**(12), 11737–11751 (2022).
42. Almusawa, H. & Jhangeer, A. A study of the soliton solutions with an intrinsic fractional discrete nonlinear electrical transmission line. *Fract. Fract.* **6**(6), 334 (2022).
43. Fahim, Md. R. A., Kundu, P. R., Islam, Md. . E. .I., Akbar, M. . A. . & Osman, M. S. . Wave profile analysis of a couple of (3+ 1)-dimensional nonlinear evolution equations by sine-Gordon expansion approach. *J. Ocean Eng. Sci.* **7**(3), 272–279 (2022).
44. Liu, J. & Osman, M. S. Nonlinear dynamics for different nonautonomous wave structures solutions of a 3d variable-coefficient generalized shallow water wave equation. *Chin. J. Phys.* **77**, 1618–1624 (2022).
45. Baber, M. Z. et al. Comparative analysis of numerical and newly constructed soliton solutions of stochastic fisher-type equations in a sufficiently long habitat. *Int. J. Mod. Phys. B* **37**(16), 2350155 (2023).
46. Niwas, M., Kumar, S. & Kharbanda, H. Symmetry analysis, closed-form invariant solutions and dynamical wave structures of the generalized (3+ 1)-dimensional breaking soliton equation using optimal system of Lie subalgebra. *J. Ocean Eng. Sci.* **7**(2), 188–201 (2022).
47. Kumar, S., Niwas, M. & Dhiman, S. K. Abundant analytical soliton solutions and different wave profiles to the Kudryashov–Sinelschikov equation in mathematical physics. *J. Ocean Eng. Sci.* **7**(6), 565–577 (2022).
48. Kumar, S. & Hamid, I. New interactions between various soliton solutions, including bell, kink, and multiple soliton profiles, for the (2+ 1)-dimensional nonlinear electrical transmission line equation. *Opt. Quantum Electron.* **56**(7), 1–24 (2024).
49. Kumar, S., Hamid, I. & Abdou, M. Dynamic frameworks of optical soliton solutions and soliton-like formations to Schrödinger–Hirota equation with parabolic law non-linearity using a highly efficient approach. *Opt. Quantum Electron.* **55**(14), 1261 (2023).
50. Abdelrahman, M. A. et al. The Exp $(-\varphi(\xi))$ -expansion method and its application for solving nonlinear evolution equations. *Int. J. Mod. Nonlinear Theory Appl.* **4**(01), 37 (2015).
51. El-Wakil, S. & Abdou, M. The extended mapping method and its applications for nonlinear evolution equations. *Phys. Lett. A* **358**(4), 275–282 (2006).
52. He, J. Homotopy perturbation method: A new nonlinear analytical technique. *Appl. Math. Comput.* **135**(1), 73–79 (2003).
53. Gu, C., Hu, H. & Zhou, Z. *Darboux Transformations in Integrable Systems: Theory and Their Applications to Geometry* (Springer, 2004).
54. He, J. & Wu, X. Exp-function method for nonlinear wave equations. *Chaos Solit. Fractals* **30**(3), 700–708 (2006).
55. Islam, M. S., Khan, K. & Arnous, A. H. Generalized Kudryashov method for solving some (3+ 1)-dimensional nonlinear evolution equations. *New Trends Math. Sci.* **3**(3), 46 (2015).
56. Gurefe, Y., Misirli, E., Sonmezoglu, A. & Ekici, M. Extended trial equation method to generalized nonlinear partial differential equations. *Appl. Math. Comput.* **219**(10), 5253–5260 (2013).
57. Hietarinta, J. Introduction to the Hirota bilinear method. In *Integrability of Nonlinear Systems: Proceedings of the CIMPA School Pondicherry University, India*, 8–26 Jan 1996. 95–103 (Springer, 2007).
58. Yan, Z. The extended Jacobian elliptic function expansion method and its application in the generalized Hirota–Satsuma coupled KdV system. *Chaos Solit. Fract.* **15**(3), 575–583 (2003).
59. Mirhosseini-Alizamini, S. M., Rezazadeh, H., Eslami, M., Mirzazadeh, M. & Korkmaz, A. New extended direct algebraic method for the Tzitzica type evolution equations arising in nonlinear optics. *Comput. Methods Differ. Equ.* **8**(1), 28–53 (2020).
60. El-Wakil, S. & Abdou, M. The extended Fan sub-equation method and its applications for a class of nonlinear evolution equations. *Chaos Solit. Fract.* **36**(2), 343–353 (2008).
61. Lamb, G. Jr. Bäcklund transformations for certain nonlinear evolution equations. *J. Math. Phys.* **15**(12), 2157–2165 (1974).
62. Zhang, J., Wei, X. & Lu, Y. A generalized $\frac{G}{G}$ -expansion method and its applications. *Phys. Lett. A* **372**(20), 3653–3658 (2008).
63. Abdou, M. A generalized auxiliary equation method and its applications. *Nonlinear Dyn.* **52**, 95–102 (2008).
64. Kudryashov, N. A. Method for finding highly dispersive optical solitons of nonlinear differential equations. *Optik* **206**, 163550 (2020).
65. Hussain, E., Li, Z., Shah, S. A. A., Az-Zo'bi, E. A. & Hussien, M. Dynamics study of stability analysis, sensitivity insights and precise soliton solutions of the nonlinear (STO)-Burger equation. *Opt. Quantum Electron.* **55**(14), 1274 (2023).
66. Li, Z. & Hussain, E. Qualitative analysis and optical solitons for the (1+ 1)-dimensional Biswas–Milovic equation with parabolic law and nonlocal nonlinearity. *Results Phys.* **56**, 107304 (2024).
67. Hussain, E. et al. Solitonic solutions and stability analysis of Benjamin Bona Mahony Burger equation using two versatile techniques. *Sci. Rep.* **14**(1), 13520 (2024).
68. Liu, J. & Li, Z. Bifurcation analysis and soliton solutions to the Kuralay equation via dynamic system analysis method and complete discrimination system method. *Qual. Theory Dyn. Syst.* **23**(3), 126 (2024).
69. Hussain, E., Shah, S. A. A., Rafiq, M. N., Ragab, A. E. & Az-Zo'bi, E. A. Exact solutions and modulation instability analysis of a generalized Kundu–Eckhaus equation with extra-dispersion in optical fibers. *Phys. Scr.* **99**(5), 055222 (2024).
70. Luo, J. & Li, Z. Dynamic behavior and optical soliton for the M-truncated fractional paraxial wave equation arising in a liquid crystal model. *Fract. Fract.* **8**(6), 348 (2024).
71. Hussain, E., Malik, S., Yadav, A., Shah, S. A. A., Iqbal, M. A. B., Ragab, A. E. & Mahmoud, H. M. A. Qualitative analysis and soliton solutions of nonlinear extended quantum Zakharov–Kuznetsov equation. *Nonlinear Dyn.* 1–16 (2024).
72. Kong, H. & Guo, R. Dynamic behaviors of novel nonlinear wave solutions for the Akbota equation. *Optik* **282**, 170863 (2023).
73. Sagidullayeva, Z., Yesmakhanova, K., Serikbayev, N., Nugmanova, G., Yerzhanov, K. & Myrzakulov, R. Integrable generalized Heisenberg ferromagnet equations in 1+ 1 dimensions: Reductions and gauge equivalence. arXiv preprint [arXiv:2205.02073](https://arxiv.org/abs/2205.02073) (2022).
74. Mathanaranjan, T., Hashemi, M. S., Rezazadeh, H., Akinyemi, L. & Bekir, A. Chirped optical solitons and stability analysis of the nonlinear Schrödinger equation with nonlinear chromatic dispersion. *Commun. Theor. Phys.* **75**(8), 085005 (2023).
75. Zayed, E. & Alurrfi, K. New extended auxiliary equation method and its applications to nonlinear Schrödinger-type equations. *Optik* **127**(20), 9131–9151 (2016).
76. Li, Z. & Zhao, S. Bifurcation, chaotic behavior and solitary wave solutions for the Akbota equation. *AIMS Math.* **9**(8), 22590–22601 (2024).
77. Malik, S. et al. Application of new Kudryashov method to various nonlinear partial differential equations. *Opt. Quantum Electron.* **55**(1), 8 (2023).
78. Phoosree, S., Khongnual, N., Sanjun, J., Kammanee, A. & Thadee, W. Riccati sub-equation method for solving fractional flood wave equation and fractional plasma physics equation. *Partial Differ. Equ. Appl. Math.* **10**, 100672 (2024).

Acknowledgements

The authors extend their appreciation to the King Saud University for funding this work through the Researchers Supporting Project number (RSPD2025R970), King Saud University, Riyadh, Saudi Arabia.

Author contributions

This work was equally contributed by all authors, and the final manuscript was approved by all authors.

Declarations

Competing interests

The authors declare no competing interests.

Additional information

Correspondence and requests for materials should be addressed to H.M.

Reprints and permissions information is available at www.nature.com/reprints.

Publisher's note Springer Nature remains neutral with regard to jurisdictional claims in published maps and institutional affiliations.

Open Access This article is licensed under a Creative Commons Attribution-NonCommercial-NoDerivatives 4.0 International License, which permits any non-commercial use, sharing, distribution and reproduction in any medium or format, as long as you give appropriate credit to the original author(s) and the source, provide a link to the Creative Commons licence, and indicate if you modified the licensed material. You do not have permission under this licence to share adapted material derived from this article or parts of it. The images or other third party material in this article are included in the article's Creative Commons licence, unless indicated otherwise in a credit line to the material. If material is not included in the article's Creative Commons licence and your intended use is not permitted by statutory regulation or exceeds the permitted use, you will need to obtain permission directly from the copyright holder. To view a copy of this licence, visit <http://creativecommons.org/licenses/by-nc-nd/4.0/>.

© The Author(s) 2025